KANSAS GEOLOGICAL SURVEY
OPEN-FILE REPORT 83-21

CRUSTAL STUDY IN KANSAS USING EARTHQUAKE SEISMOGRAMS

by

Richard D. Miller

Disclaimer

The Kansas Geological Survey does not guarantee this document to be free from errors or inaccuracies and disclaims any responsibility or liability for interpretations based on data used in the production of this document or decisions based thereon. This report is intended to make results of research available at the earliest possible date, but is not intended to constitute final or formal publications.

Kansas Geological Survey
1930 Constant Avenue
University of Kansas
Lawrence, KS 66047-3726

CRUSTAL STUDY IN KANSAS USING EARTHQUAKE SEISMOGRAMS

by

Richard D. Miller
B.A., Benedictine College, 1980

Submitted to the Department of
Physics and the Faculty of the
Graduate School of the University
of Kansas in partial fulfillment
of the requirements for the degree
of Master of Science.

Professor in Charge

Committee Members

For the Department

ABSTRACT

Seismic refraction studies have been used for about three decades to explore continental crustal structure. In this thesis a refraction study was done using regional earthquakes with epicentral distances of 300 kilometers or greater in place of explosions as energy sources. Analysis of earthquake seismograms from the eastern Kansas earthquake network resulted in the location of several acoustic discontinuities within the crust in central and eastern Kansas. Calculated Pn velocity is consistent with previous studies in the area. A higher velocity crustal acoustic discontinuity below CNK, SNK, TCK and MLK determined through Pn residual calculations is assumed to be related to the Precambrian aged Midcontinent Geophysical Anomaly (MGA). An omnidirectional positive Pn residual zone centered on EDK may be related to the Wichita geomagnetic low. Pn time residuals at CNK and SNK show delays possibly related to the presence of the arkosic Rice Formation in northeastern Kansas. Directionally dependent apparent Pn velocities indicate a Mohorovicic discontinuity dip to the west, north, and south from the study area but is relatively flat to the east. A Pn velocity of 8.25 km/sec $\pm$0.15 km/sec seems consistent throughout the network. Error analysis reveals that layer depths and thicknesses cannot be accurately

determined with data presently available in Kansas Geological Survey record archives.

TABLE OF CONTENTS

LIST OF TABLES

LIST OF FIGURES

ACKNOWLEDGEMENTS

I would like to extend my deepest graditude to my advisor and friend, Dr. Don Steeples, whose guidance and support from conception to completion of this thesis was invaluable. Thanks to my other committeemen, Dr. Ralph Knapp and Dr. Dan Ling for their helpful suggestions and comments en route to completion of this manuscript. Thanks also to Shlomo Shmuelov for his design and implementation of the digitizing software. I would also like to acknowledge the help received from Renate Hensiek in the preparation of illustrations. To Jeanie Joyce, a special thanks for her assistance in compiling the rough draft version of this thesis.

Finally, I would like to recognize the numerous members of the Kansas Geological Survey staff who lent their support and special skills throughout; especially, Brett Bennett and Esther Price.

INTRODUCTION

Determining a crustal model that most nearly resembles the earth's true crust, with respect to all its physical properties, has been an area of interest to earthquake seismologists since epicentral locations were first attempted. The more precisely the earth's crust and upper mantle can be modeled, the greater is the degree of accuracy and integrity associated with defining regional seismic trends. Some attempts to better define the earth's crustal structure were made early in earthquake seismology using phase arrivals (Byerly, 1946). These phase arrivals represent refracted energy propagating along discrete crustal layers.

In recent years, explosion seismology has been more extensively used for crustal modeling. Refraction surveys using explosives permit investigators to exercise control over the elements that induce the largest error in direct analysis of earthquake arrivals: source location, origin time, receiver array, and area of study (Steinhart and Meyer, 1961).

Without a good crustal model, foci locations lack a narrow zone of convergence resulting in a misleading data set for identification of seismic epicenters. The best technique for crustal modeling, closely

exemplifying the propagation paths earthquake energy traverses, results from analysis of distinct earthquake seismograms with well-constrained foci locations; however, in order to get good foci locations a good crustal model is necessary. At this point the circular logic that faces the seismologist becomes evident (Pakiser, 1963). Refraction modeling through direct analysis of earthquakes on seismograms in conjunction with preliminary crustal models obtained through conventional seismic refraction profiles ultimately should result in a representative crustal model.

GEOLOGIC SETTING

The area monitored by the Kansas Earthquake Network and under investigation here, is contained within the Central Stable Region (Snyder, 1968). The generalized transcontinental crust is made up of a silicic upper layer covering a mafic lower layer (Pakiser and Zeitz 1965). The stable environment of the midcontinent shows relatively thick crust (approximately 50 km) with lower crustal P-wave velocities in the 6.7 km/sec range, generally representative of a gabbro, and the upper mantle rocks show P-wave velocities in excess of 8.0 km/sec and relatively high density (Pakiser, 1963).

The region under study here contains many major upper crustal structural features, some of which show the effects of activity in deeper layers (fig 1). The origins of these features are not clearly defined; however, it has been proposed that during the late Precambrian an extensive series of geologic events occurred (Snyder, 1968). These events began with long periods of igneous activity over the entire midcontinent resulting in the formation of the Keweenawan basin. This was followed by renewed igneous activity and the development of the major fault lineament (Midcontinent Geophysical Anomaly) dividing the midcontinent. Subsidence, uplift, and erosion was continued throughout

Paleozoic with the gradual formation of the basins and arches.

This sequence of events was in part responsible for the major structural features of the Precambrian basement distinquished by drill data (Cole, 1976). The Precambrian surface in northern Kansas is composed of a wide variety of igneous and metamorphic rocks (Bickford et al., 1979).

The major Precambrian-aged feature from a geophysical viewpoint, in the Central Stable Region is the Midcontinent Geophysical Anomaly (MGA). The MGA extends laterally from Lake Superior (where the rocks that cause it do outcrop) through Kansas into Oklahoma (Yarger, 1983 in press), and represents a +60 mgal gravity high flanked by -100 mgal lows which are dissected in several places by possible transform faults (Chase and Gilmer 1973). In Kansas, the MGA is a structure with suggested upper mantle presence (Hahn, 1980). The magnetic and gravity influence of the MGA is seen quite clearly (Yarger 1980, Yarger 1983 in press). A potential fields model of the MGA by Yarger (1976) correlates a high density and highly magnetic rock body with geologic data from Bickford et al., 1979 (fig 2). Previous studies have suggested a connection between density variations, similar to those found across the

MGA, and velocity anomalies in the crust (Press and Biehler, 1964).

The MGA apparently is a result of Keweenawan-aged plate tectonic interaction. The geologic and geophysical characteristics of the MGA show a great deal of similarity to the seven well known rift and ridge systems and it has, therefore, been classified as a rift system. It was interpretively named the Central North American Rift System in accordance with this classification (Ocola and Myer, 1973). The MGA terminology used here is not interpretive in nature and leaves open the possiblility of other geologic causes such as the possible trace of a Precambrian-aged "hot spot".

The Nemaha Ridge is another of the major structural discontinuities in the study area. There is seismic reflection evidence to suggest major uplifting during late Mississippian time which produced the Nemaha Ridge, forming the boundary between the Salina and Forest City basins in Kansas (Steeples, 1982).

Aside from the MGA and Nemaha Ridge, there are several other structural features that could have some acoustical significance to this thesis. Of most importance are those that lie between the foci and the receiver points and include the following: Ozark

Uplift, Sioux Uplift, Central Kansas Uplift, Forest City Basin, Anadarko Basin, and Salina Basin.

The crustal environment below 1.5 km has been investigated predominantly using geophysical techniques. Deep crustal structure has been determined primarily with the use of regional refraction techniques and gravity modeling (Steeples, 1976),(fig 3). The crust of north central Kansas and eastern Colorado showed three dominant acoustic discontinuities: a 4.5 km/sec layer from 1/2 km of depth to about 1.3 km, a 6.0 km/sec layer from 1.3 km to about 8.1 km of depth, and a 6.1 km/sec layer from 8.1 km of depth to the Mohorovicic discontinuity (Moho). At the crust/mantle interface a gentle eastward thinning of crust is observed with a depth of 38 km $\pm$6 km at the east end of the refraction line and upper mantle velocity of 8.25 km/sec (Of course the energy penetration associated with this velocity is extremely shallow into the mantle.)

Refraction studies of crustal structure have been conducted at the fringes of the study area. Tryggvason and Qualls (1967) and Mitchell and Landisman (1971) in central Oklahoma depict a flat-layered crust with a 46 km and 51 km depth to Moho, respectively, giving some idea of the uncertainty involved in interpretation of refraction data. Stewart (1968) analysed refraction

lines that extend through central and southern Missouri (fig 3). Results from that study estimate average Moho depth from 42 km on the western end of the central Missouri line decreasing to 38 km on the eastern end. Apparent Pn velocities in central Missouri ranged from 8.1 to 7.9 km/sec. On the southern Missouri line depths to Moho range from 45 km in the West with an apparent velocity of 8.0 km/sec to 38 km in the East with an apparent velocity of 8.2 km/sec.

Recent investigation of deep crustal structure, in the study area, was undertaken by the Consortium for Continental Reflection Profiling (COCORP) in 1979 with preliminary interpretation done by Brown et al. (1983). The seismic lines were planned in such a way as to sample subsurface points related to significant geophysical or geological features. The structural features of particular interest to the investigators were the Nemaha Ridge, MGA, and the Humboldt fault. In addition to investigation of these features, deep crustal structure was a primary target of the study.

Past refraction profiling has modeled the deep crust of Kansas as layered with discrete velocity discontinuities relating to continuous, homogeneous beds of great lateral extent (Steeples, 1976). In fact, the structure below 12 km is characterized by discontinuous,

heterogeneous dipping layers, with varying thickness (Brown et al., 1983). In the small area being studied by COCORP, deep reflection techniques show regions with possible large granitic intrusions and acoustically transparent zones. The two way travel times where these steeply dipping discontinuous reflectors, with random reflection zones beneath, appear is at about 3-4 sec (9-12 km). Below these granitic intrusions are acoustically significant layers with complex reflection patterns, many assumed to be from outside the plane of the survey. The granitic-to-gabbroic rock interface may be of sufficient acoustic impedence contrast to cause the relative high reflectivity observed throughout this zone of apparent complex structure.

The COCORP investigation in Kansas has been unable to show a vivid continuous reflector from the 11-13 sec (34-38 km) zone which is the expected arrival time for the crust/mantle interface (Moho) throughout the survey area in Kansas. However, the character of energy returning from below the assumed Moho reflector zone has subtle irregularities and trace-appearance differences. The assumption is that these character changes are in some way related to the Moho.

Other geophysical and geological techniques lack sufficient regional accuracy to have application in

crustal modeling. In particular, the use of gravity as an aid in determining shallow crustal density variation is a valid technique; but the use of gravity in large scale crustal structure analysis would not necessarily lead to a concise model (Pakiser, 1963).

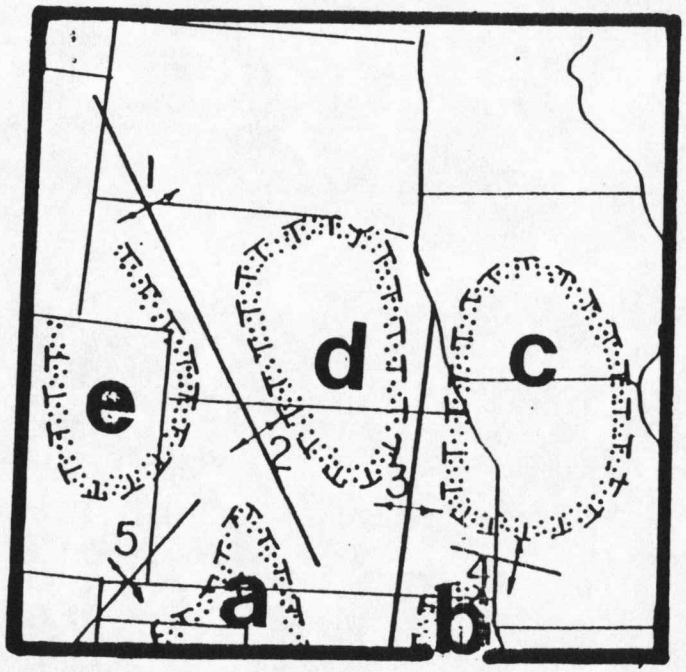

Uplifts

1. Cambridge
2. Central Kansas
3. Nemaha
4. Bourbon
5. Las Animas

Basins

a. Hugoton
b. Cherokee
c. Forest City
d. Salina
e. Denver

Fig. 1. Major structural features within the study area as described by Snyder (1968).

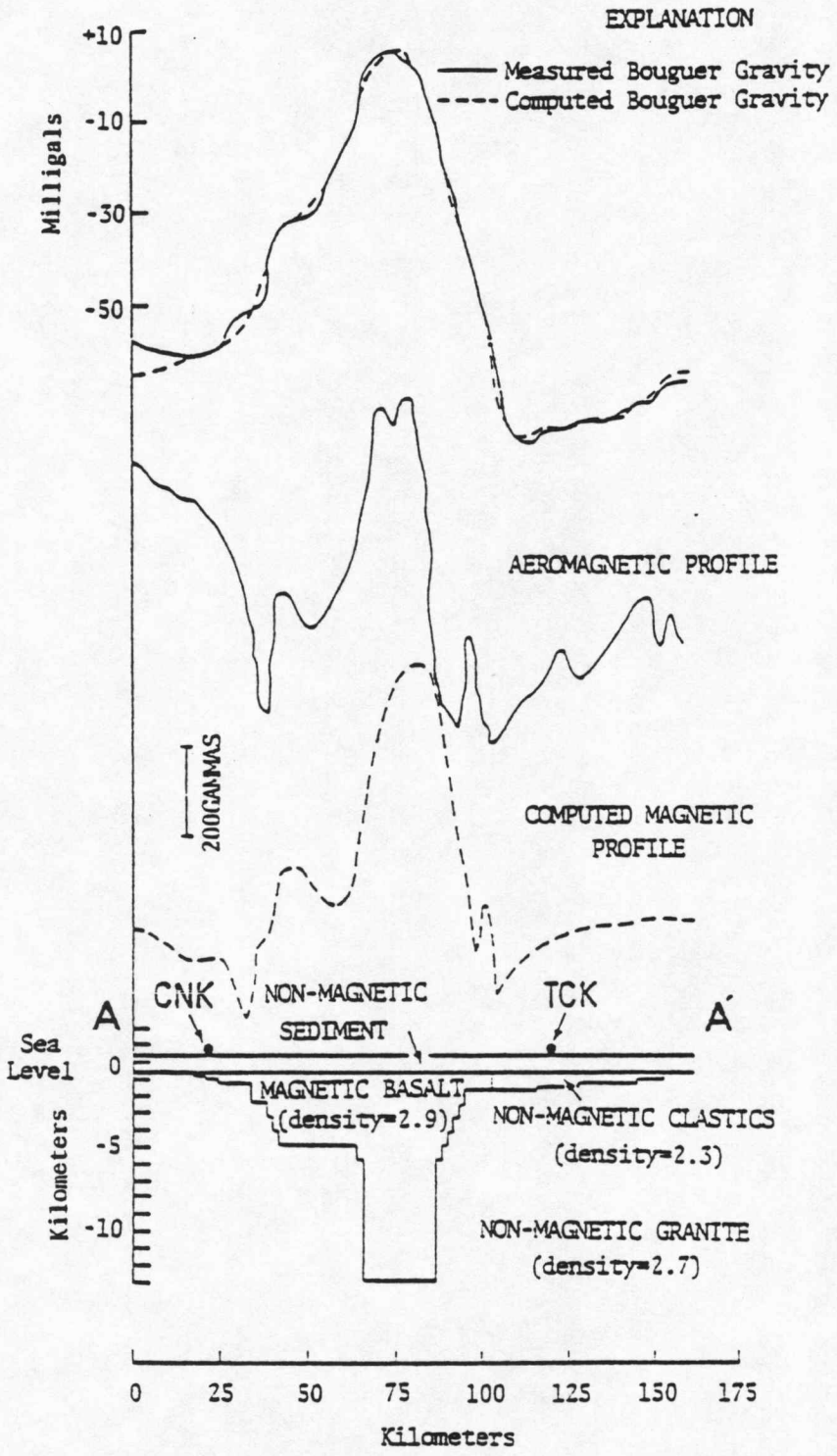

Fig. 2. Crustal cross-section derived from east-west magnetic and gravity profiles across the MGA from 96.15° to 98.0° W. longitude at 39.5° N. latitude. (After Yarger, 1980, in Hahn, 1980).

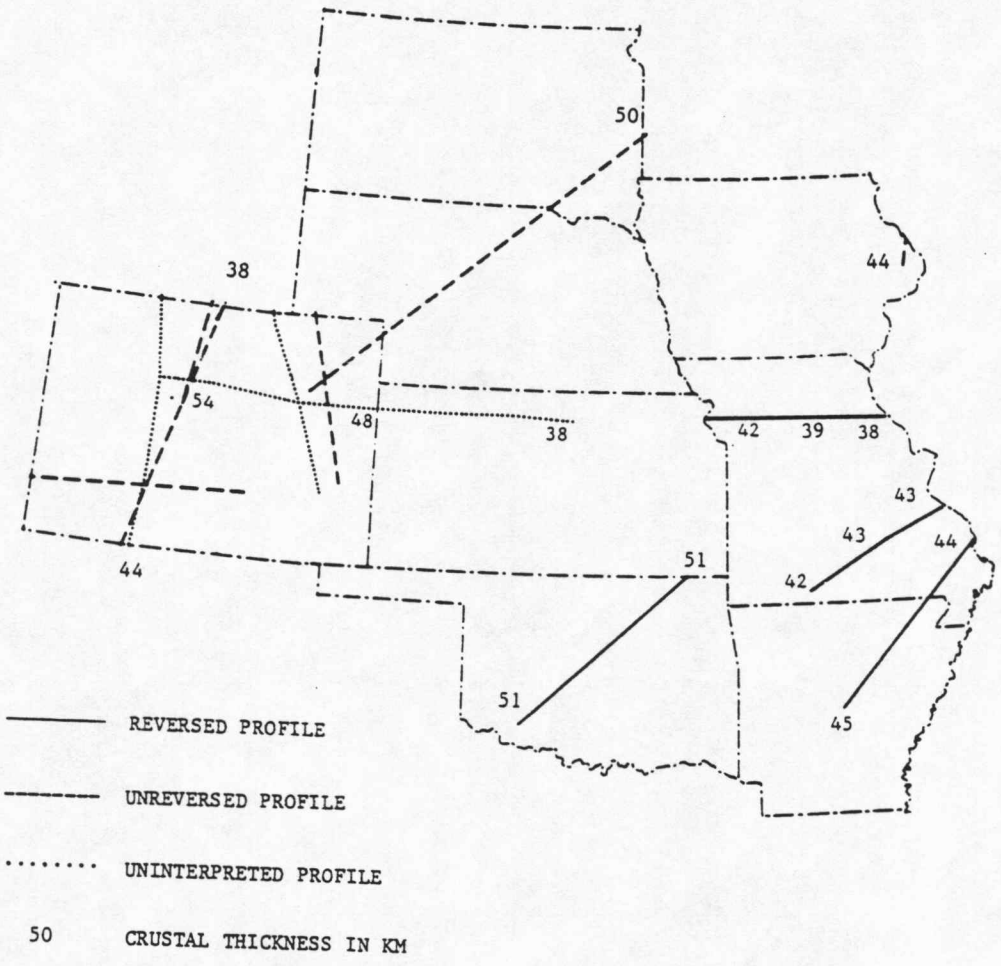

Fig. 3. Location of previous seismic-refraction profiles in or near the study area and their associated calculated depths. Consolidated from maps in Warren and Healy (1973).

WAVE THEORY

Refraction Technique

A wave train interacting with an ideal homogeneous acoustic boundary within the earth can classically behave in any one or combination of the following ways: reflection, refraction, or transmission (in accordance with Snell's Law). The exact behavior of a wave after it contacts an interface depends mainly on the angle of incidence. Energy travelling downward in a wave train that contacts a velocity discontinuity at the critical angle, will refract and then (after physical compensation for the new environment) propagate through the lower medium. Waves behaving in this fashion are referred to as "head waves". After refraction head wave velocity is dependent upon the type of particle motion incident on the refracting horizon. A compressional head wave has an oscillatory motion in the direction of propagation and parallel to the refractor (Telford et al., 1976). This oscillatory motion is present in both the upper and lower media, due to the obvious fact that relative motion between two media deep in the earth is not possible. At the boundary both media are forced to move in phase with each other. Part of the total energy being transported by the head wave continuously emerges from just below the refractor at the critical angle.

Earthquake energy critically refracted at the crust/mantle interface must travel at least the critical distance of the Pn phase between source and receiver. Here in the central midwest waves originating from earthquakes less than approximately 210 km distant do not show all the necessary distinct phase arrivals representative of a multilayered crust. There are two factors that dictate the value of the Pn phase critical distance: depth to the crust/mantle interface and velocity ratio of the lower crust and upper mantle. Geometrically, this is seen from examination of the time/distance curves of refracted, reflected, and direct waves travelling through the media. Knowing all the discrete energy arrivals representative of velocity discontinuities is critical in the formulation of an accurate earth crustal model.

With the station array concentrated in eastern Kansas, in a somewhat circular distribution, refraction studies using the stations lack the 2-dimensional precision that is present using line arrays, as in conventional refraction studies. However, by using a great circle technique of station alignment, the regional features should have only minor distortion, assuming proper sampling. This technique, however does average out any subtle or localized geologic features.

Wave Types

According to classical wave theory, energy can propagate through an elastic medium as either of two wave types: body waves (compressional waves or transverse waves) and surface waves. The characteristics that govern the type of wave motion propagating through an elastic medium are: particle displacement, relative frequency, and environmental factors (such as depth in the earth, density of material, velocity of propagation, existence of layering, etc.). Separating waves by the previous characteristics makes the classification of all energy propagating through the earth possible. On earthquake seismograms, energy arrivals are the products of constructive and destructive interference of phases through multiple refractions, reflections, and mode conversions.

Phase Description

According to wave theory, body waves propagating from a single point source in a homogeneous, isotropic medium disperse their energy as $1/r^2$ from that source. In a medium with several velocity discontinuities propagation of energy may result in the arrival at a

point of several energy packets of the same wave type (particle motion) originating at the same instant, but travelling different paths. The relative time separation of these arrivals depends on depth to refractor, distance between source and receiver points, dip of discontinuities, homogeneity of dip, and presences of localized velocity anomalies. This results in a series of compressional wave arrivals followed by a group of translational wave arrivals. These discrete compressional and translational wave arrivals are known as "phases". There are three widely used and identified phases of both compressional and shear waves: Pn, P*, and Pg as well as Sn, S*, and Sg. These different phases are associated with discrete paths the energy follows to get from source to receiver (fig 4).

Individual phase arrivals are defined by Pakiser (1963). He defined four different compressional waves (Pg, P*, Pn, $\bar{P}$).

Pg, a compressional wave that has penetrated through the sedimentary veneer of the earth and travels as a refracted wave in the upper layer of the crust at a velocity of about 6.0 km/sec. Amplitude of Pg typically falls off exceedingly rapidly with distance.

P*, a compressional wave that has penetrated through the upper layer of the crust and travels as a refracted wave in a deeper layer of the crust at velocities ranging from 6.5 to about 7.0 km/sec.

Pn, a compressional wave that has penetrated through the crust and travels as a refracted wave in the upper mantle rocks at velocities ranging from 7.7 to about 8.2 km/sec.

$\bar{P}$, a guided wave that travels in the upper layers of the crust with a velocity near that of Pg. $\bar{P}$ is especially well developed at distances larger than the crossover from Pg to Pn, where the amplitude of Pg is frequently too small to be detected.

These definitions originated from conventional refraction profiles with surface sources (Pakiser,1963).

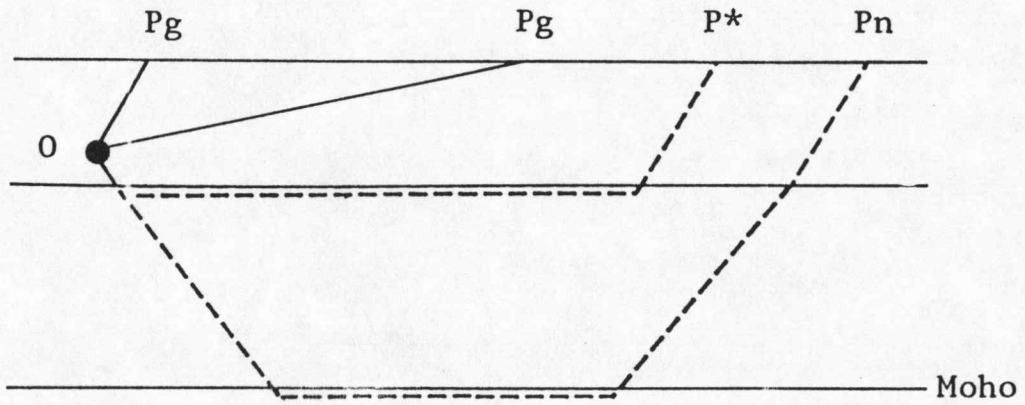

Fig. 4. Paths of major compressional waves through the crust.

NETWORK

The earthquake network in Kansas began operation at its present level of sensitivity in December, 1978. At that time the network consisted of six stations installed, operated, and maintained by the Kansas Geological Survey (KGS). Funding for the stations was provided by the United States Nuclear Regulatory Commission (NRC) and the Kansas City District, Army Corps of Engineers. The Kansas network was designed for the study of seismic activity along potentially active geologic features in eastern and central Kansas. In April of 1979, three stations were added by the KGS. Support for these additional central Kansas stations was provide by the NRC (fig 5).

The present 9-station network was designed, engineered, and installed to optimize location potential of microearthquakes in eastern Kansas which is classified as a medium risk zone. Station sites were chosen in an effort to avoid excessive cultural interference and ensure a good signal to noise ratio. The network possesses the sensitivity necessary to locate events with duration magnitude as low as 1.5 in the eastern half of Kansas (Sheehan and Steeples, 1983, in press).

Each station is equipped with a telemetry system,

power supply, and seismometer. The seismometers are at the bottom of cased boreholes 50-58 meters deep. The seismometers were placed at the bottom of the borehole in an effort to use the earth's own filtering characteristics to attenuate much of the low amplitude surface noise, particularly at frequencies of 10 Hz or higher.

Signal from each of the 9 stations is transmitted via long distance, voice-grade telephone lines to the KGS. Once at the KGS, the signals are discriminated, amplified, filtered, and displayed on analog paper records using pen-and-ink rotating-drum seismographs. Through this process, the signal is filtered twice, once in the field and once in the lab. This filtering process has a 0.05 sec or less phase delay in signal arrival at the drum recorder's pen (Hahn, 1980). The records are then scanned, analyzed if necessary, and archived for future reference.

For the majority of the life of the Kansas Earthquake Network the seismometers have been Teledyne Geotech S-500's. The S-500 operates with the use of a piezoelectric quartz crystal and amplifier which produce a voltage representative of velocity in earth particle displacement.

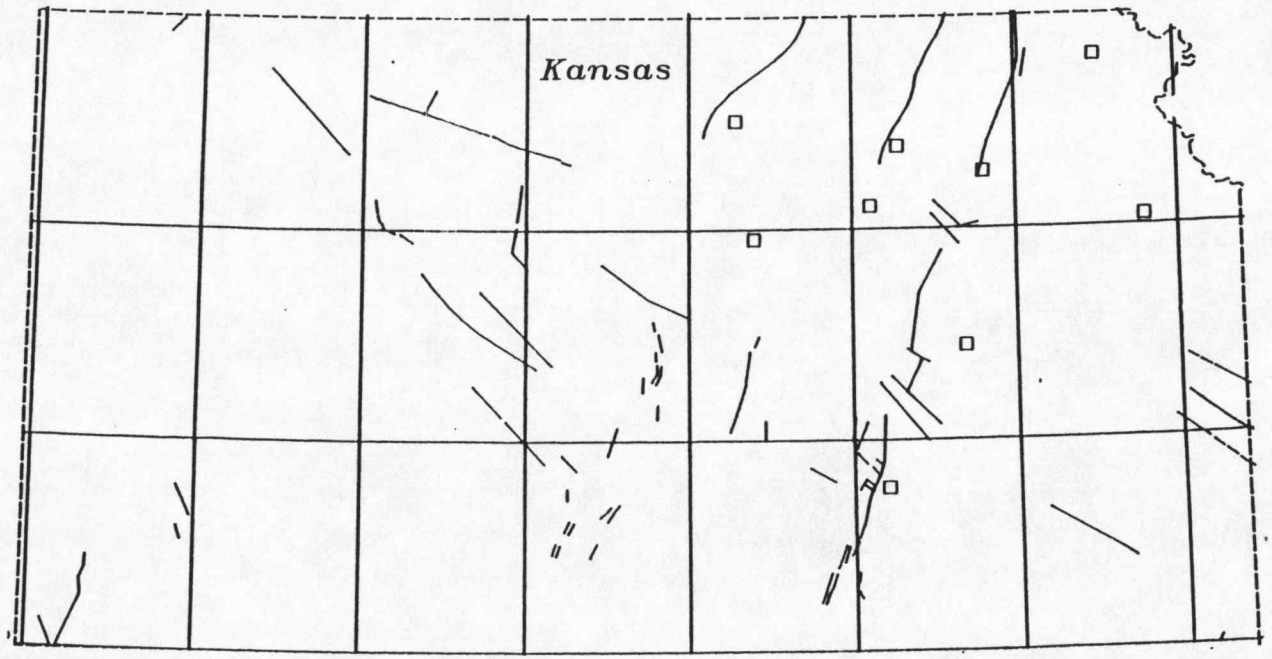

Fig. 5. Kansas Geological Survey's earthquake stations in conjunction with mapped faults. (□ = station locations; / = faults)

DATA ANALYSIS TECHNIQUE

Phase Picking

The picking of intermediate phases originating from assumed discrete velocity discontinuities, consolidates two fundamental schools of thought. One school represents earthquake phase identification as an "art", the other displays the picking of earthquakes on seismograms by following a very precise scientific method. Generally, the picking and timing of events recorded on analog seismograms is a subjective procedure. Many attempts have been made to reduce the subjectivity associated with the picking of first energy arrivals of intermediate phases, but with little success (Borcherdt, 1968).

Velocity determinations are strictly relative measurements of the time taken to travel from one receiver location to another (for the purpose of this thesis all receivers have been translated along great circles until they align with the source-receiver lineament). After absolute timing is established (WWV radio broadcasts of Coordinated Universal Time (UTC)) incorporation of origin time and comparisons of travel time curves can be made. Any ambiguity resulting from absolute timing errors can be reduced through first arrival shifts.

Picks of impulsive first break energy (Pn) inherently carry more integrity than picks of energy arrivals later in the wave train (Pakiser et al., 1964). This is because of the interference of a second arrival with the decaying first break, and so forth for the third, fourth, fifth, ... arrivals. These later arrivals may interfere constructively or destructively, resulting in phase amplitude and arrival time distortion (modulation).

Individual phases are recognized by a series of physical characteristics that distinquish that phase from the rest of the wave train (fig 6). These characteristics can be any one or any combination of wave character, amplitude variations, or frequency changes. Pakiser et al. (1964) described the picking of phases in the following way:

> Identification of events follows circular reasoning: an event is assumed to represent a particular layer when it arrives at the time expected for the regional model, and the time of the event is then used to verify the model.

Amplitude and frequency changes represent physical properties that are less dependent on human judgment and have more concrete evidence for a chosen energy arrival. Character changes as a criterion for picking an arrival are much more dependent on personal experience in

scanning events (art) than on other discrete identifiable variations. However, character changes, when used in conjunction with the other techniques is a viable means of distinquishing arrivals.

The identification of intermediate phases, from events farther than the Pn critical distance, implies something inherent about the crustal model expected. It clearly negates the possibility of a crust having a smooth, gradational velocity change with depth. When picking discrete arrivals following Pn, one clearly assumes unique origins for the time-staggered energy arrivals, not necessarily continuous in lateral extent, representing defined velocity discontinuities.

Each wave packet (from first break of Pn to first break of Pg) contains multiple apparent discrete arrivals. Distinquishing true refracted energy arrivals from bogus arrivals depends on continuity between seismograms and linear correlation of arrival times with epicentral distance. Continuity of phase arrivals from one event to the next is a criterion of extreme importance in the formulation of directionally dependent apparent velocity models. Because this factor weighes so heavily in the determination of an accurate model, bias can be present in the sorting of possible phase arrivals. However, no pick was made without clear

indication of either character, frequency, or amplitude change resembling that expected from true energy arrivals on a seismogram.

Different P phases generally do not maintain the same apparent physical appearance thoughout the wave packet. Because of this character change, more bias enters into the picking and categorizing of phase arrivals. Also, because the environmental and electronic variations from station to station, energy arriving at different stations from the same refractor many have distinctly different physical characteristics. However, between stations some frequency information is usually retained and this helps to give some integrity to the arrivals chosen.

At this point, the subjectivity involved with picking true intermediate energy arrivals becomes apparent. One way of maintaining some continuity in phase arrivals, from one record to the next, is through the use of a current crustal model. With the existing model as a guide, it is possible to determine approximate arrival times for the Pg-wave. The existing model used (Steeples, 1976) is a two layer crust representing the earth response to energy propagating through it. The anticipated arrival pattern from the psuedo discrete layers of the crust should have three

distinct phase arrivals. First break energy relates to Moho refractions (Pn). Second arrivals result from critical refractions at the 8 km acoustic discontinuity. Finally, the Pg arrival is indicative of the direct wave and should lag the Pn arrivals by (Pg-Pn here defines travel time difference):

$$\frac{\text{Epicentral Distance} - 229}{25.4} = \text{Pg-Pn}.$$

Previously described energy arrival patterns on the seismograms would only be applicable at distances greater than the crossover distance of Pn. Intermediate phases are distinguished by the relative positon of their arrival within the distance varying Pg-Pn time span.

This analysis technique has excellent potential for determining the apparent velocity and depth of the acoustic discontinuity associated with $\bar{P}$ phase. This phase is difficult to distinqish from Pg at distances less than the cross-over from Pg to Pn (Pakiser, 1963). In many cases, intermediate phases never appear as first arrivals, at least in continental regions, and they must be inferred from later arrivals at distance greater than Pn critical distance (Eaton, 1966).

Depth Determination

An attempt was made to calculate apparent layer depths using earthquake arrivals as unreversed refraction profiles. Using the equation for an n-layered non-dipping crust as required by the existing data, typical depth errors were in the range of ± 20 km. The apparent depths are not indicative of true depth; but, are a constraining mechanism for grouping apparent velocities according to apparent depth of refracting horizons. These calculations also help one to disregard an apparent velocity due to an unrealisitic depth of the associated acoustic boundary. Use of depth values for determination of true depth to a velocity discontinuity was abandoned because of the large error.

Digitizing

Data for this study were recorded using paper analog records. Due to complex appearance of the data, lack of a suitable means of presentation of the data, and an economical means of consolidating multiple events, manual digitizing of each phase arrival was performed. Each prepicked and timed discrete phase arrival point was digitized but wave forms were not digitized. Each phase arrival is represented by a

spike, with height relative to the amplitude and certainty of that particular phase. Display is in standard record section format. Thus the seismogram is simplified to show only interpreted picks of appropriate amplitude, devoid of noise and waveform complications.

The digitizing process was done with a Tektronix 4052 microcomputer interfaced to a 4956 digitizing table and a 4909 hard disc. The software package was created exclusively for this project by Shlomo Shmuelov.

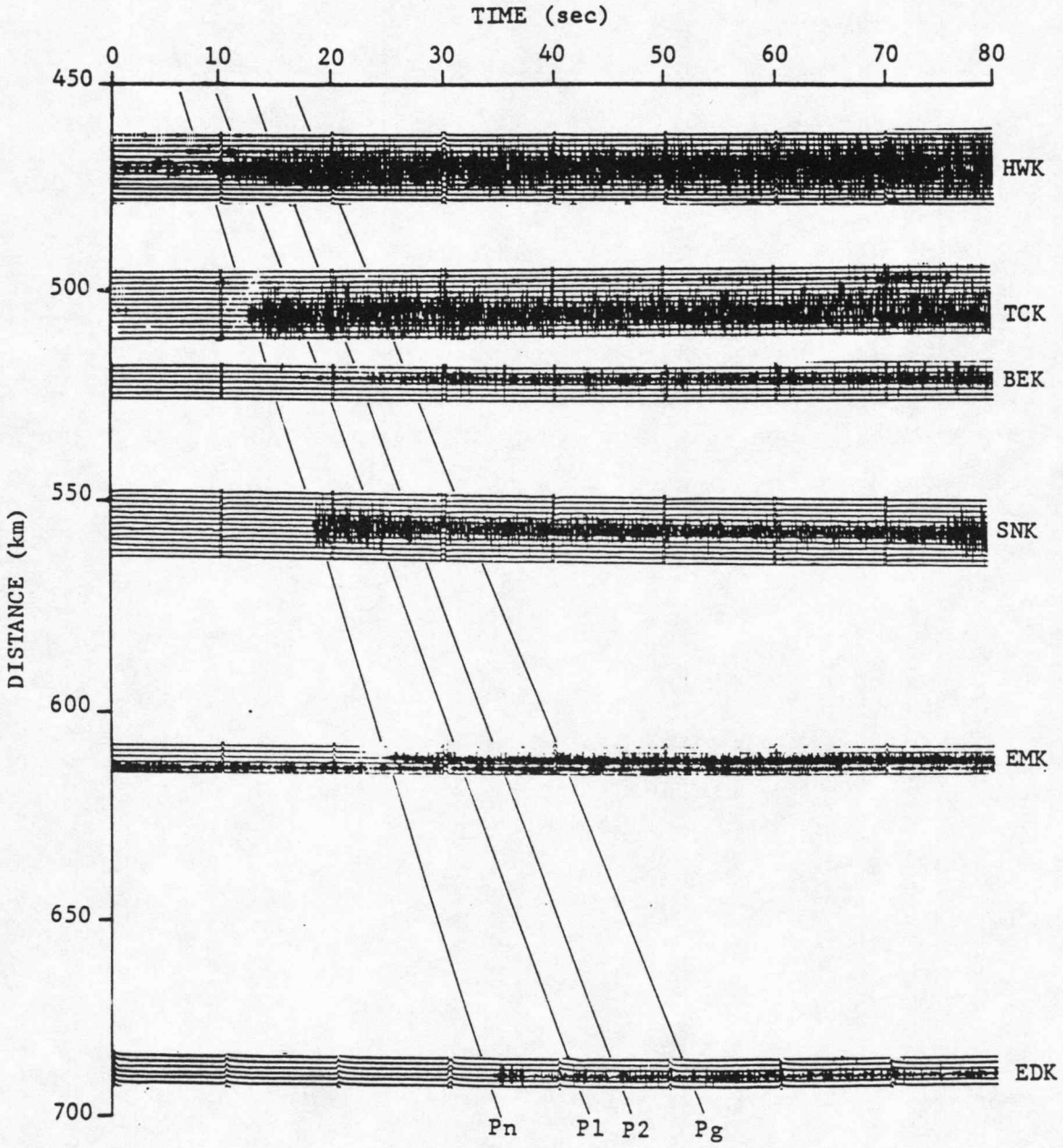

Fig. 6. Time/Distance curve of event 13 representative of the data set showing some of the physical characteristics used to distinguish phase arrivals.

ERROR ANALYSIS

Precision of epicenter location controls the inherent accuracy of the refraction model. Focal parameters needed to determine a meaningful crustal model include longitude, latitude, origin time, and depth. The sources of these values were the United States Geological Survey (USGS), St. Louis University, and the Oklahoma Geophysical Observatory. St. Louis University and the Oklahoma Geophysical Observatory rely on crustal models in the location of epicenters and origin time. However, the USGS uses world-wide characteristic travel time curves in their location routine.

Due to the regionally more precise location method using crustal models, whenever parameters from St. Louis University or the Oklahoma Geophysical Observatory could be used, they were. These events typically have maximum surface location errors of about 2 km in diameter. The remaining location errors (i.e. events north and west of the KGS network) with epicentral distances determined from the USGS listing, could be as large as 10 km. The errors associated with the epicentral parameters must be carried through to the final model with no hope of reducing them (at least in-house).

Locations by the Kansas Geological Survey were not

possible in most cases due to the extreme source to receiver distance. All events studied here were around 300 to 500 km away from the closest KGS station, making the azimuthal gap too great to give an accurate, stable solution.

A very important parameter in refraction modeling is origin time determination. From an Oklahoma Geophysical Observatory printout and Central Mississippi Valley Earthquake Bulletin location, maximum origin time fluctuation expected is generally ±1.0 sec. The USGS listings can have as much as ±3.0 sec of deviation in origin time.

Another parameter associated with refraction profiling which has the potential for significant error, is depth to source. For the area under study, the focal depth of most events ranges from 5 to 15 km with an uncertainty of about 10 km. Depth to source has considerable control over refractor depth determination. Errors of 10 km represent origin time shifts of as much as 2 sec. A 2 sec shift in origin time will change the calculated Pn refractor depth 8 km or more depending on velocity and upper layer characteristics (table 1). The combination of these sources of error produces the depth uncertainties that led to the abandonment of depth calculations as discussed earlier.

Velocity errors of secondary arrivals are not only dependent on epicentral parameter errors, but also on timing errors associated with proper identification of secondary phase first breaks, actual timing of picked phase arrivals, and error associated with synchronization of clocks to Coordinated Universal Time (UTC). The previously mentioned areas that error enters into a velocity calculation have the following impact:

1) improper identification of phase ±0.25 sec,
2) precision of hand timing process ±0.05 sec,
3) clock synchronization accuracy ±0.05 sec.

Grouping all these velocity error windows together, a total maximum timing uncertainty of ±0.35 sec, is obtained. This timing uncertainty was calculated for intermediate phase arrivals. Pn wave arrivals don't have the ±0.25 sec window associated with picking the proper instant, at least for events that are not emergent. This ±0.25 sec figure can be replaced by ±0.10 sec value relating to locating the first break of an emergent wave. So, when dealing with first break Pn arrivals, a timing uncertainty of ±0.20 sec is contained within the process, while intermediate phase timing invokes a ±0.35 sec window of uncertainty.

Correlation of phase is a very individualized segment of the total error. Each event has its own characteristic subsurface anomalies that distort the picking and interpreting of phase arrivals. It is difficult to give numerical windows of error for correlation discrepancies. Misinterpretation of apparent phases relates back to picking arrivals that conform to a previously conceived crustal model.

A comparison of the arrivals chosen to represent phases from five different events, two from the south and three from the east, is the data set used to give insight into the precision of phase correlation. The three events from the east were from Arkansas. The epicenters had maximum separation of 9 km. They are one major shock and two after shocks, and have a smaller location uncertainty than was given earlier. The two events from the south are from Oklahoma with epicentral separation of 33 km.

For the southern events (8 and 9) there is a Pn velocity variance of 0.1% and an intermediate phase variance of about 2.0%. Pg shows a 3.2% variation in correlation. The eastern events (2, 3, and 4) have a Pn velocity variance of 1.7%, an intermediate phase percent error of 2.0%, and Pg phase variance of 7.0%. As discussed earlier the Pn phase contains the smallest

inherent timing errors of any phase arrivals at distances beyond the Pn cross-over distance.

In most cases significantly poor correlation of phases from event to event dictates the disregarding of the arrival of certain events. Throughout the compressional wave train many phase arrivals that seem prominent may not be the result of energy travelling uninterrupted along an acoustic boundary.

A numerical weighting routine is a rudimentary means of giving some indication of the certainty of individual picks. Along with each timed phase arrival is a value representative of the picker's confidence in the arrival chosen. Zero is highest confidence while four indicates the time should not be used in velocity determinations at all.

Velocity uncertainties are the consequence of errors and ambiguities previously indicated. Because velocity calculations are determined by the slope of a line, origin time shifts are not relevant. To obtain an accurate velocity error value, consideration of both location errors and timing errors must be made. Calculated Pn velocity errors induced by USGS, Oklahoma, and St. Louis epicentral location errors are on the order of ± 0.01 km/sec and are insignificant relative to other sources of error in this study. Pn velocity

errors associated with timing are a result of the ±0.20 sec uncertainty previously determined. This timing uncertainty is approximately ±0.15 km/sec. For intermediate P-wave arrivals an additional 1.0 sec error must be included to compensate for lack in coherent identification of phases. With this inclusion the uncertainty for intermediate arrivals is approximately ±0.30 km/sec.

To summarize the foregoing error analysis, errors are so large that they precluded any layer depth calculations and limit discussion of intermediate crustal layers to qualitative velocity analysis. Neither a crustal model nor an intermediate P-wave residual model can be derived with the existing precision. Pn arrivals contain sufficient accuracy to use confidently in calculations performed in this thesis.

TABLE 1

I. UNITED STATES GEOLOGICAL SURVEY'S P.D.E. LISTINGS

Parameter	Uncertainty (Pn) Distance	Time
* Epicentral distance	±5 km	±0.75 sec
* Focal depth	±10 km	±1.6 sec
* Origin time		±3.0 sec
TOTAL		±5.35 sec

II. OKLAHOMA GEOPHYSICAL OBSERVATORY AND CENTRAL MISSISSIPPI VALLEY EARTHQUAKE BULLETIN.

Parameter	Uncertainty (Pn) Distance	Time
** Epicentral distance	±1 km	±0.15 sec
** Focal depth	±5 km	±0.80 sec
** Origin time		±1.0 sec
TOTAL		±1.95 sec

* Personal Communication.
** Published data accompanying bulletin.

DATA ANALYSIS

Analysis of first breaks is one of the more accurate means of refracted compressional wave analysis; however, it is not the only valid technique available for crustal studies using refracted compressional waves. Secondary phase arrivals contain information worthy of consideration. As described in an earlier section, each phase arrival associated with P-wave refracted energy can be timed and used in a fashion similar to first break energy.

From a comparison of several good quality events arriving at the network from the same general direction, certain acoustic properties and apparent structural anomalies of the crust and upper mantle can be identified.

In the development of travel time curves, one event from each direction is chosen as a guide event, with the remaining events from that direction being time shifted such that the Pn phase arrivals align as closely as possible to the guide event's Pn arrival. Events are shifted as units, effectively correcting for the poor depth-of-focus control in this regional earthquake analysis. Guide events are selected after consideration of location precision, correlation of phase arrivals, repeatablity with other local events, compatiblity with conventional reversed refraction profiles in the area, and

the author's own judgment concerning each event's quality.

Events 8, 9, 10, 11, and 12 were located by the Oklahoma Geophysical Observatory and have general progression patterns from south-southwest into the network with epicentral distances ranging from 365 km for the closest station to about 900 km for the most distant station with discernible phase arrivals. Event 9 was chosen as guide event, which dictated a -1.0 sec shift in event 8, a -1.5 sec shift in event 11, and a -3.0 sec shift in event 10. After alignment, the 5 south events were plotted together (fig 7). Events 8 and 9 are two events that show very similar wave train character (fig 8). An apparent velocity of 8.35 km/sec $\pm$0.15 km/sec for the crust/mantle interface recorded by these two events is a velocity within experimental error of previously obtained values (Tryggvason and Qualls, 1967). Arrival of P1 phase energy shows an apparent velocity across the network of 7.45 km/sec $\pm$0.30 km/sec. Propagation of energy across the network at an apparent velocity of 6.71 km/sec $\pm$0.30 km/sec is identified as P2 wave. The Pg wave has an apparent velocity of 6.21 km/sec $\pm$0.30 km/sec.

Other events from the south originated from the Texas Panhandle region. Event 12 has features that closely resembled the two model Oklahoma events (8 and 9). The slight variation in values might be associated with

gradual regional changes in crustal thickness and upper crustal heterogeneities. Comparison of events 8, 9, and 12 gives a model with a larger subsurface sampling. This model, however, would not show the proposed Moho low in central Oklahoma (Warren et al., 1973). All phase arrivals from event 10 (not used) lack good correlation and show significant irregularities in apparent velocity. This lack of correlation is probably associated with phase identification errors.

Complex structure dominates the upper crust between the eastern events and the recording network (Stewart, 1968). Apparent velocity as determined from some eastern events shows consistant first break data (table 2). Event 2 was chosen as the alignment event; therefore, event 1 was shifted 1.6 sec, event 3 was shifted -0.7 sec, event 4 was shifted 0.2 sec, event 5 was shifted 0.3 sec, and event 7 was shifted 1.5 sec (fig 9).

Events 2, 3, and 4 were used as indicative of the subsurface to the east (fig 10). These events show good Pn velocity agreement within themselves, with an average of 8.21 km/sec $\pm$0.15 km/sec. These events have epicenters in the Mississippi Embayment. Earthquakes that originate from outside a concentrated grouping in northeastern Arkansas lack regional consistency and are used predominantly for station residual determinations.

Events 2 and 4 indicate an apparent velocity of 7.57 km/sec ±0.30 km/sec for an energy arrival identified as P1. P2 for these two events shows a 7.01 km/sec ±0.30 km/sec apparent velocity. Event 7 originated in Tennessee and shows significant similarity to events 2 and 4 from Arkansas, increasing the likelihood of a representative eastern crustal model.

Event 1 has an apparent Pn velocity of 8.38 km/sec ±0.15 km/sec. Event 1 also has a P1 apparent velocity of 7.38 km/sec ±0.30 km/sec.

Event 6, originating in Kentucky, contained sufficient energy to saturate the analog recorders. All significant information beyond excellent first break energy was clipped. Event 6 has an epicentral distance greater than any other studied here. After rejection of LAK and EDK from the data set due to poor correlation to the least squares line, an apparent Pn velocity of 8.87 km/sec ±0.15 km/sec was obtained from about 1000 km from the source to at least 1860 km.

Previous studies in the Midcontinent have documented a 9.27 km/sec ±0.05 km/sec velocity at a source/receiver offset of 1700 km (Masse, 1973). Comparing the Pn apparent velocity and source/receiver offset of event 6 to that of Masse's refraction lines shows some distinct simularities. Masse has a Pn crossover for his lines

around 130 km; in my study area a 229 km Pn crossover previously established (Steeples, 1976) could explain variations that are present between the two studies. A 328 km depth was calculated for the 9.27 km/sec refractor by Masse.

Events 13, 14, and 15 are the northern data set. These three events have epicenters with horizontal separation between events 13 and 15 of approximately 580 km and between events 13 and 14 of 149 km. Event 13 was used as a guide event and as a result, event 14 experienced a 2.5 sec time shift and event 15 was not used (fig 11). From the values for intermediate P velocities and y intercepts misjudgments concerning phase identification were made. The wide spatial separation of these epicenters probably caused a lack of good intermediate arrivals that can be consistently picked from event to event.

Events 13 and 14 have apparent Pn velocities that show good consistency and very little deviation. For that reason the apparent Pn velocity for the northern crust is formulated predominantly using events 13 and 14 (table 2). The Pn apparent velocity from the north is 8.38 km/sec $\pm$0.15 km/sec. Pg phase arrivals from the north are consistent from event to event with an average value of 6.21 km/sec $\pm$0.30 km/sec.

As characteristic of many seismic refraction surveys when applying statistical techniques, lack of sufficient data poses a sizeable difficulty in interpreting data on travel time curves (Borcherdt et al., 1968). This problem was encountered in dealing with energy arrivals originating in the west. Only one event falls within the limits of the previously conceived guidelines for data acceptance. From event 16, an apparent Pn velocity of 8.59 km/sec $\pm$0.15 km/sec was calculated. Later phase arrivals have inconsistent data in comparison to other values from the entire region under investigation.

Velocity Model

In determining a velocity model, a high quality data set of sufficient size to obtain a distribution that averages to the true apparent velocity is critical. Small data sets are characteristic of refraction surveys, whether from explosion sources with economic contraints, or from natural earthquake energy with nature's own recursion limitations. Therefore, events that conform to preconceived error limits and have consistency with other events in the proximity, are consolidated into one time/distance curve representing the apparent velocities from the general direction (north, south, etc.) being sampled (fig 7, 9, and 11).

In some cases correlation of points on time/distance curves is poor. If travel time picks have been made in a highly consistent manner, shifts in time necessary to align velocity curves are essentially a correction for differing source depth and source depth errors (Mooney, 1982). Due to poor depth convergence on hypocentral locations, some depth values are assigned according to localized assumed focus depths. In order to compensate for this scatter of velocity curves when comparing multiple events from the same direction, a technique commonly known as an apparent velocity plot across the stations (technique coined from explosion seismology) is used in conjunction with an unshifted time/distance curve. Again as previously noted, plotting off-line stations as linear distributions assumes a homogeneous crust and may mask or eliminate localized anomalies.

Apparent velocity models represent the speed with which each head wave travels across the network. This suggests that the only area sampled is that between the source and receiver and a subsurface size equivalent to that of the network, at the critical angle from the surface station array. Consistency of phase arrivals dictates the status of individual events in the formulation of an apparent velocity model.

In an area of dipping beds and nonhomogeneous layers

apparent velocity does not represent true velocities. Determination of true velocity must be done with reverse profiles.

Residuals

The calculation of residuals is implemented with the assumption that the least squares determined slope is the true apparent velocity for the layer. Then with the use of the equation for a line, residuals (i.e., the amount of time a phase arrival deviates from the straight line approximation of the apparent velocity of propagation) are calculated by the following equation:

$$\text{Residual} = \text{Arrival Time} - \frac{\text{Epidistance} - \text{Y Intercept}}{\text{Velocity}} .$$

From the residuals, characteristic directional delays or early arrivals for each station can be identified. Certain stations show consistently late or early arrivals, depending on crust and upper mantle anomalies. Using a statistical approach of determining directional delays enables interpretation of velocity anomalies and apparent unconformities within the subsurface sampling area.

As a head wave propagates across the network, it can interact with anomalous velocity zones that originate

and/or terminate within the network. If heterogeneities of this sort exist, energy propagation across the network will be nonlinear in time. The size of the residual is dependent on size of the anomalous zone, velocity contrast between zones, and orientation of the zone with respect to raypath propagation of energy from the crust/mantle interface:

$$\Delta t = \frac{\Delta h \ (V2 - V1)}{(V2 * V1)} ,$$

where Δt= residual, Δh= anomalous material path length, V2= velocity of anomalous material, and V2= velocity of surrounding crustal material.

Only Pn phase arrivals have sufficient calculated accuracy to be used confidently in residual calculations in this study. Pn arrivals, also by definition, penetrate all layers of the crust. Therefore, any anomalous zone within the crust of the subsurface network area, should be encountered by this wave as it propagates toward the surface at its critical angle.

Reversed Refraction from Oklahoma

Reversed refraction profiles allow accurate depth and velocity determinations of individual acoustic boundaries

that propagate a head wave. To implement a reversed refraction profile it is essential to have events with sufficient energy originating from within or just outside two receiver arrays (earthquake networks) offset by at least the Pn crossover distance along with synchronization of time.

Simultaneous analysis of the June 30, 1979 earthquake in Kansas and the September 14, 1979 earthquake in Oklahoma proved fruitless. The recorded amplitudes of the arrivals from these events are not large enough to provide reliable phase picks. The result of the attempt at reversed refraction analysis was a geologically and geophysically unrealistic model. The only useable information resulted in conformation of the direction of Moho dip.

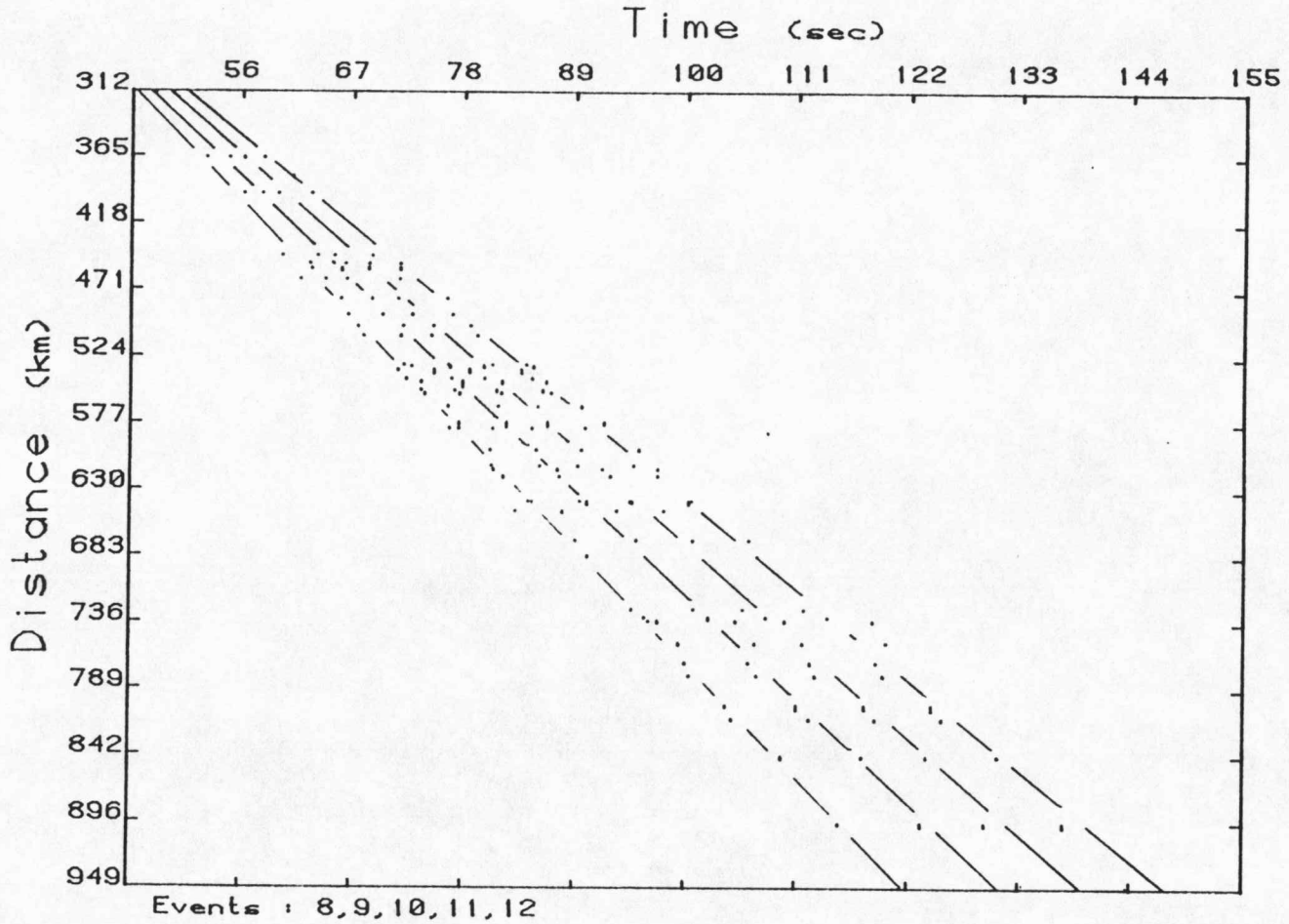

Fig. 7. All events from the south used in the formulation of the residual model.

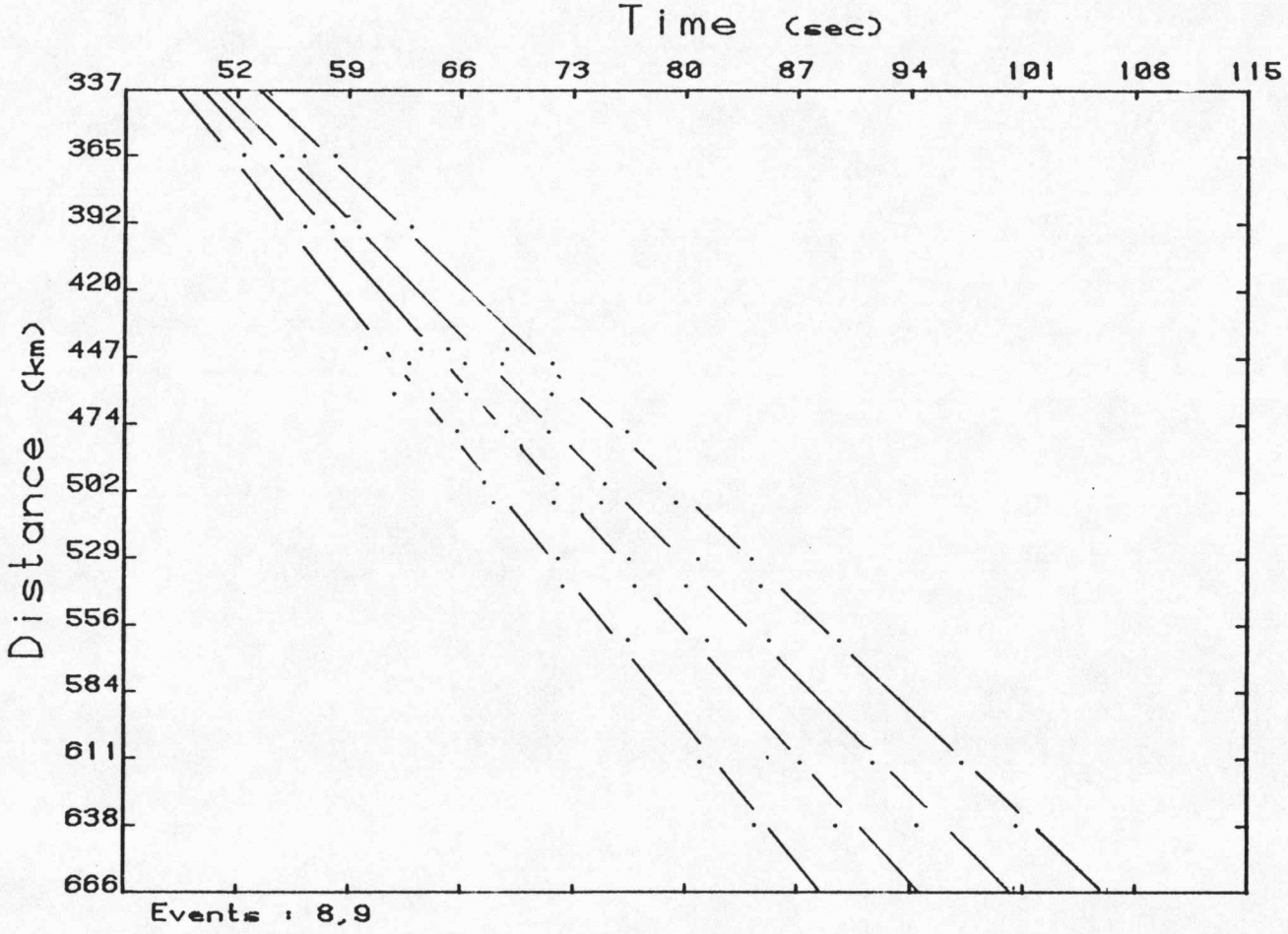

Fig. 8. Events from the south used to determine correlation of phase.

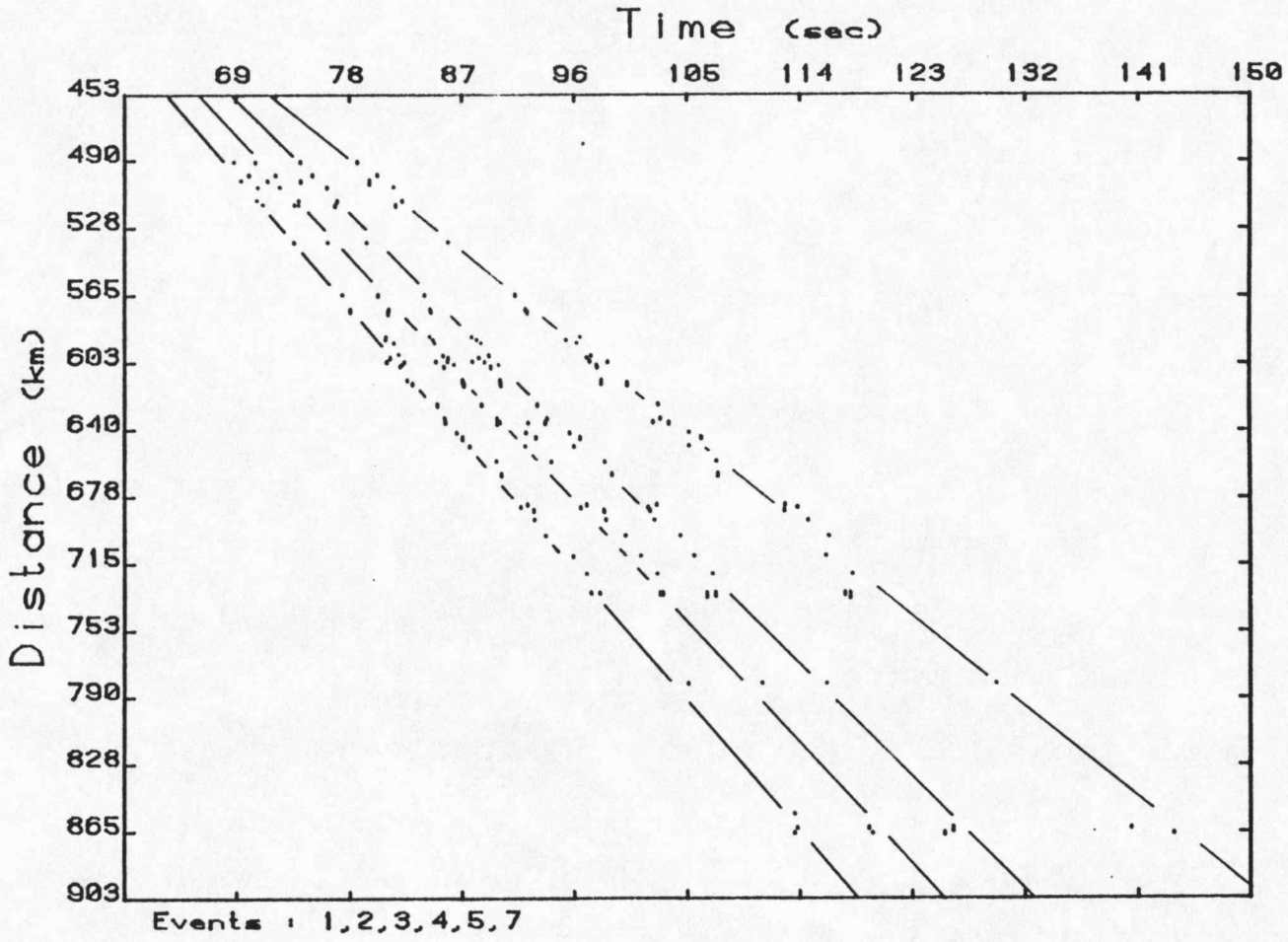

Fig. 9. All events from the east used in the formulation of the residual model.

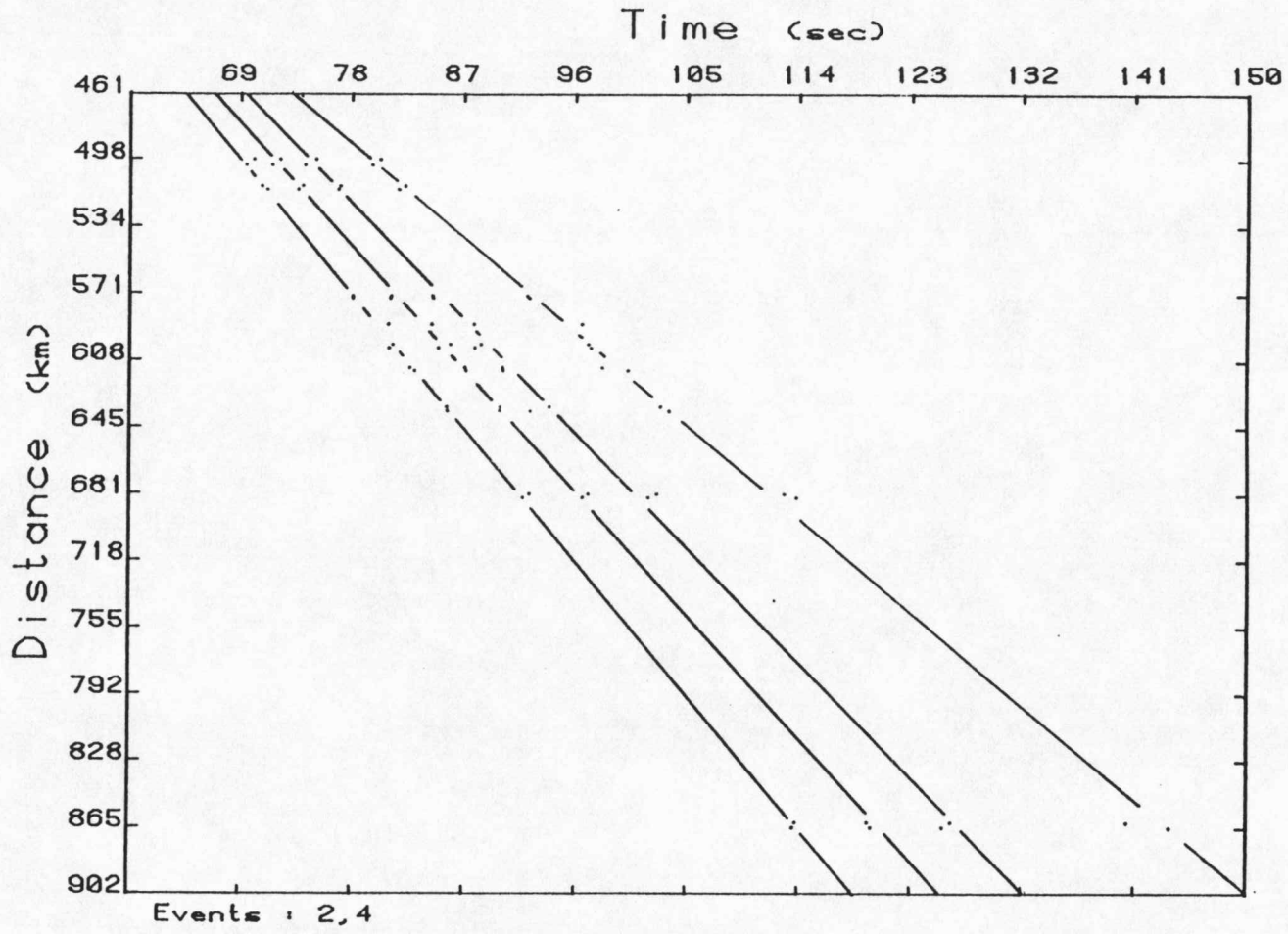

Fig. 10. Events from the east used to determine correlation of phase.

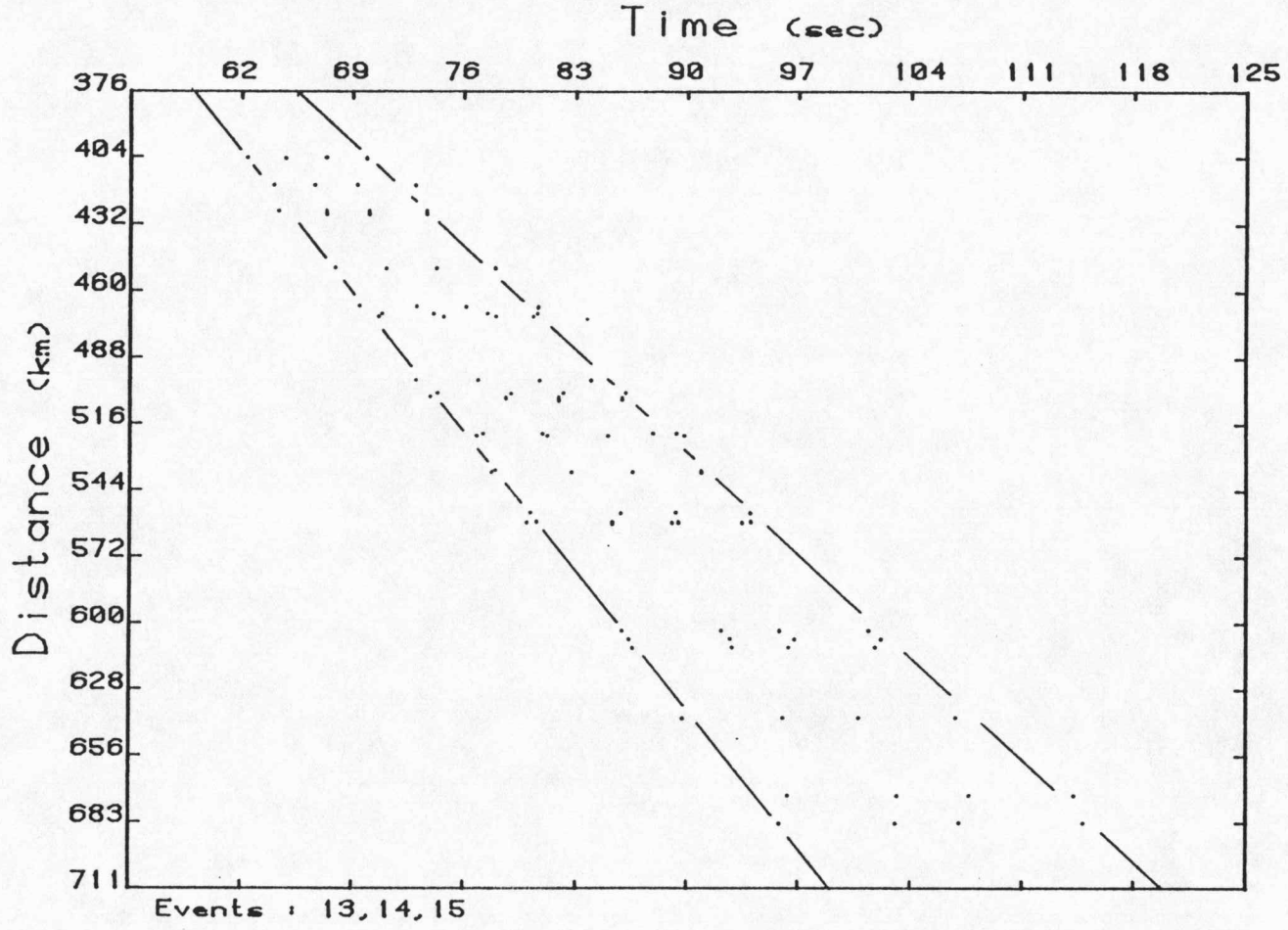

Fig. 11. All events from the north used in the formulation of the residual model.

TABLE 2

APPARENT VELOCITY MODEL

South

PHASE	EVENTS	APPARENT VELOCITY*	STD. DEVIATION*	RELATIVE RANGE*
Pn	8,9,11	8.33 ± 0.15	0.026	0.05
Pl	8,9,11,12	7.41 ± 0.30	0.085	0.20
P2	8,9,11,12	6.73 ± 0.30	0.063	0.15
Pg	8,9,11	6.28 ± 0.30	0.104	0.19

East

Pn	2,3,4,7	8.18 ± 0.15	0.084	0.19
Pl	2,4	7.58 ± 0.30	0.106	0.15
P2	2,4,5†,7	7.03 ± 0.30	0.026	0.06
Pg	1,2,3,4,5,7	5.74 ± 0.30	0.207	0.59

North

Pn	13,14	8.38 ± 0.15	0.028	0.04
Pg	13,14	6.21 ± 0.30	0.075	0.15

* km/sec

† (Originally interpreted as Pl phase, but correlates with other events better as P2 phase.)

DISCUSSION

Using earthquakes as the energy source for refraction surveys restricts much of the control over the data set that is present on conventional refraction profiles. On the other hand using multiple events with different epicenters provides more complete sampling of the subsurface. In this fashion, a more representative model showing the lateral extent of velocity anomalies can be obtained from deeper layers that intersect the anomalous material.

Within the crust, complex reflection patterns from COCORP data have been hypothesized to be the result of either gneissic banding, interlayering of granite and restites relating to anatexis, or mafic intrusions (Serpa et al., 1983). Gabbro intruding into granite (assumed to be representative of the basement geology associated with the MGA) and forming an anomalous velocity zone could have sufficient lateral and vertical extent to cause velocity anomalies similar in magnitude to those experienced here. A complex crust, could have characteristic phase arrivals from intermediate beds that could have velocities and depths covering a sizeable range of values. Depending on the degree of change over distance, events from the same general direction could show extreme distortion in the interpreted layering calculated from prominent refracted

wave arrivals.

From analysis of apparent velocities originating from different directions, approximate trends in layer dip can be determined. Also from an apparent velocity, determination of directional station delays can be done. Station delays could indicate anomalous velocity zones or crustal heterogeneities possibly representative of previous tectonic activity or vulcanism. Complex structure results in multiple interactions with anomalous velocity zones which complicates the interpretation. Direct application of directional station delays to earthquake location routines could tighten the margin of error presently noticeable in even the best locations using a regional crustal model.

Interpretation of a nonhomogeneous crust using Pn residuals here depends greatly on one key assumption. That assumption is that a least squares fit to the data is a sufficient mean for making relative comparisons of station arrivals.

From Pn residuals there is evidence to suggest an anomalous high velocity crust in the northwestern portion of the network (fig 13). The presence of such a velocity anomaly has been suggested in previous studies (Lui 1980, Serpa et al., 1983).

Modeling of an anomalous high density crust was

completed using gravity and aeromagnetic data collected over the proposed high velocity crust (Yarger,1980) (fig 2). Good correlation can be found between the potential field model and the seismic velocity delay model.

Transition of a P-wave from a granitic crust, which is commonly accepted as the predominant crustal rock type in the area, into a basaltic environment could give velocity residuals similar to those experienced here. The size of the residual, of course, is also dependent on height of the anomalous rock column. Exact determination of boundaries using the existing station array is not possible; however, an approximate minimum surface distortion pattern can be established. Boundaries can be estimated using the stations within the anomalous material as control points for a minimum affected area. In general the anomalous high velocity area includes CNK, SNK, MLK, and TCK (fig 13).

Also suggested is the presence of a low velocity boundary material on the west flank of the velocity high. Correlation of this velocity delay zone with previously determined structural features yields possible ties to the arkosic Rice Formation (Precambrian). Also, there are hints of stray patches of anomalous crust in the central part of the station array.

From the north, assuming the model derived to be

correct, TCK, MLK, CNK, and SNK should be early with the other stations showing zero or late residuals. The actual data show some residual scatter about the network. Arrivals at EDK show delay, with HWK and LAK also arriving later than average. Phase arrivals at CNK, EMK, SNK, and TCK are slightly early with respect to the other stations arrivals (fig 12). Without more and/or better data, interpretation of the north epicenter residuals lacks good scientific basis; however, grouping of residuals as seen here, would indicate a pattern possibly developing. The early arrivals are consistently located at stations in the north-central and northwestern part of the network.

The south should show the anomaly by early arrivals at CNK, SNK, TCK, and MLK with late or zero residuals at BEK, HWK, LAK, EMK, and EDK. The residuals show good consistency, with the southern stations EMK, EDK, and LAK being late and stations CNK, SNK, MLK, HWK, and TCK showing relative early arrivals (fig 12). With this type of distribution, a lineament can be placed through the network dividing early and late arrivals. This lineament could possibly be indicative of some discontinuity within the crust or upper mantle, between the subsurface origin points and surface receivers of EDK, EMK, and those of SNK, MLK, and HWK. This could be indicative of and related to the major east-west crustal collision zone

proposed by Yarger (1981) on the basis of aeromagnetic patterns. HWK arrivals from the south are part of the evidence for anomalous material possibly located within a station triangle of BEK, LAK, and EMK.

Events from the east have ray paths that could intersect the anomalous low velocity upper mantle at the Moho as previously identified by Hahn (1980). With this in mind, arrivals from the east might be expected to show at TCK, MLK, and SNK early with CNK and the remainder of the stations showing late. These events have a more complex residual distribution than those from the south. Again EDK has an unquestionable delay, with HWK and CNK having late arrivals, as well. MLK and TCK tend to have earlier than expected arrivals (fig 12). A higher velocity crustal material beneath TCK and SNK could influence the arrivals resulting in deviatons from the average as experienced here. It is likely that higher velocity crustal material is present beneath these stations because of the mafic rocks associated with the MGA. The late CNK reading may result from the slowing of the Pn head wave as it passes through the anomalous low velocity zone originally defined as the root of the MGA (Hahn, 1980).

The event from the west, if it shows the same anomalous zone, will have SNK, CNK, MLK and TCK early with

BEK late, and the rest of the stations will be zero or at least earlier than BEK. BEK's late arrival could be expected from an interaction with a low velocity mantle.

The lone event from the west has good consistent residual values with respect to the southwestern events which are compatable with delays determined on a previous study (Lui, 1980) (fig 12). SNK and CNK have a very profound late arrival. These late arrivals could be related to the same feature. The most physically and geologically reasonable explanation relates to Pn-wave penetration of the Rice Formation located west of the surface station locations. The Rice Formation is a large deposit of arkosic material with P-wave velocity less than that of granite or basalt. Early arrivals were found at MLK and TCK, which seems to be a consistent situation for energy propagating across the network from all directions. Again a late arrival is the rule for EDK, with a delayed arrival at EMK and BEK as well.

After delays are calculated, it is obvious that EDK always records Pn arrivals late with respect to the calculated mean (table 3). In order to compensate for what appears to be either a very localized anomaly or just physical characteristics of EDK, a station correction of 0.3 sec was subtracted from all Pn times at EDK. For the most part, this station correction affected the final

interpretation of the delays very little.

A 0.3 sec station correction was applied to HWK and TCK, one station having consistently early arrivals and one station having an arrival pattern consistent with that calculated as representative of the data set. This correction was made in order that relative shifts in residuals could be studied and more insight gained into the nature of the early arrival zone.

Analysis of near-regional events, most showing source/receiver offset less than the Pg-Pn crossover distance, does not result in any significant delays in first break energy that would contradict the interpretation presented here. However, it must be kept in mind that residuals calculated by earthquake location programs are not exactly analogous to values determined by comparison of actual arrival times with expected times calculated from the least squares velocity.

Consistently late arrivals at EDK from regional events could be related to a geophysical anomaly, previously detected and its borders defined by an aeromagnetic study of Kansas (Yarger et al., 1980). The anomaly is represented by a low of 600 gammas, centered near EDK. A continental collision zone has been given as a possible explanation for the low (Yarger, 1981). Rock types at the Precambrian surface in the area lack any

evidence for the presence of this aeromagnetic low (Bickford, 1979). However, it has been suggested that some type of plate convergence process could have been operational during mid-Proterozoic time (Van Schmus et al., 1980). Local event residuals do not suggest the presence of low velocity material in the upper part of the crust. The arrival time patterns observed are therefore consistent with both the shallow Precambrian geology of Bickford et al. (1979) and Van Schmus et al. (1980) and the hypothesized collision zone of Yarger (1981).

Examination of Pn residuals from event 6 (from Kentucky) suggests possible evidence for a low velocity upper mantle near the MGA. TCK and MLK show slightly late arrivals with respect to the least squares apparent velocity for the first break compressional wave recorded. With an assumed 328 km velocity discontinuity as the source of the critically refracted head wave the propagation path could intersect part of the hypothesized low velocity, upper mantle root of the MGA (Hahn, 1980) in Kansas.

Comparison of figures 7 and 9 shows distinctly different arrival character associated with the Pg phase. The eastern events show a much slower upper crustal velocity. This could be the result of a non-isotropic layer in the upper crust. Speculation aside, the Pn, P1,

and P2 phase arrivals show slope and arrival spacing similar to events from all directions. However, the Pg phase arrivals from the east show a spacing and slope unique to that direction of propagation.

Exact determination of a crustal model using this technique and data set has not proven to be totally successful. However, a great deal of possible subsurface structure previously unrevealed through compressional wave arrival studies, was analysed and partially resolved here. Certain characteristics (amplitude of intermediate arrivals, frequency of impulsive head waves, etc.) of the P-wave arrivals studied showed dependence on the area and direction from the station array the energy originated from. Assuming gross consistency in characteristic velocities a general direction of layer dip can be qualitatively assigned from apparent velocities.

As a result of the apparently complex crust in the study area, discrete intermediate P-wave arrivals originating from the same layers in all directions could not be confidently identified. Generally, Pn-wave identification and timing were sufficiently accurate for a Moho velocity in the study area to be calculated. There seems to be sufficient evidence to suggest that the Moho dips away from the study area to the west, north, and south and seems to level off to the east. The velocity of

the upper mantle is approximately 8.25 km/sec ±0.15 km/sec, within the network.

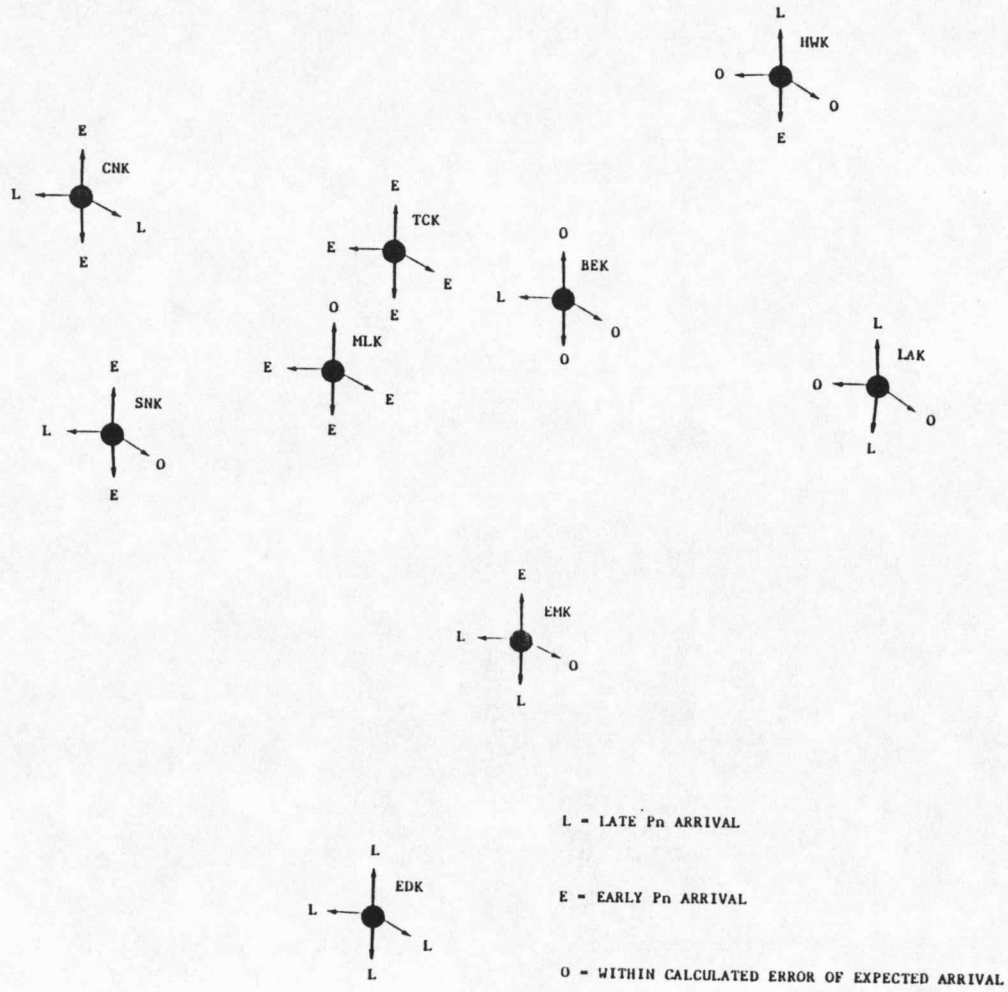

Fig. 12. Pn phase arrival residuals classified relative to expected arrival times calculated from the directional average apparent velocity across the network.

TABLE 3

AVERAGE RESIDUALS

No Station Corrections

	STD	TCK	MLK	BEK	SNK	CNK	HWK	LAK	EMK	EDK
NORTH	(.37)	-0.2	0.0	+0.1	-0.2	-0.4	+0.5	+0.2	-0.2	+0.2
SOUTH	(.53)	-0.2	-0.2	+0.1	-0.5	-0.4	-0.2	+0.5	+0.3	+0.4
EAST	(.32)	-0.3	-0.2	-0.1	0.0	+0.2	+0.1	0.0	+0.1	+0.4
WEST	(.72)	-1.0	-0.8	+1.1	+0.6	+0.6	-0.1	-	+0.3	+0.4

After EDK -0.3 Sec station Correction

NORTH	(.38)	-0.3	-0.1	+0.1	-0.2	-0.4	+0.5	+0.2	-0.1	0.0
SOUTH	(.51)	-0.1	-0.1	+0.3	-0.4	-0.3	-0.2	+0.5	+0.5	+0.2
EAST	(.31)	-0.4	0.0	-0.1	-0.2	+0.4	+0.2	0.0	+0.1	+0.2
WEST	(.71)	-1.1	-0.9	+1.0	+0.4	+0.5	-0.2	-	+0.2	0.0

After HWK -0.3 Sec Station Correction

NORTH	(.33)	-0.1	0.0	+0.2	-0.2	-0.3	+0.3	+0.4	-0.2	+0.2
SOUTH	(.56)	-0.1	-0.4	+0.2	-0.5	-0.3	-0.3	+0.6	+0.5	+0.3
EAST	(.33)	-0.4	-0.3	-0.1	+0.1	+0.3	+0.1	0.0	+0.1	+0.8
WEST	(.73)	-1.1	-0.9	+1.0	+0.4	+0.4	-0.5	-	+0.2	+0.3

After TCK +0.3 Sec Station Correction

NORTH	(.34)	-0.1	-0.1	+0.1	-0.5	-0.4	+0.6	+0.3	-0.1	+0.2
SOUTH	(.51)	+0.1	-0.5	0.0	-0.4	-0.4	-0.2	+0.3	+0.4	+0.3
EAST	(.31)	-0.1	-0.3	-0.2	-0.1	+0.2	+0.2	0.0	0.0	+0.3
WEST	(.65)	-0.8	-0.9	+1.0	+0.4	+0.5	-0.2	-	+0.2	+0.3

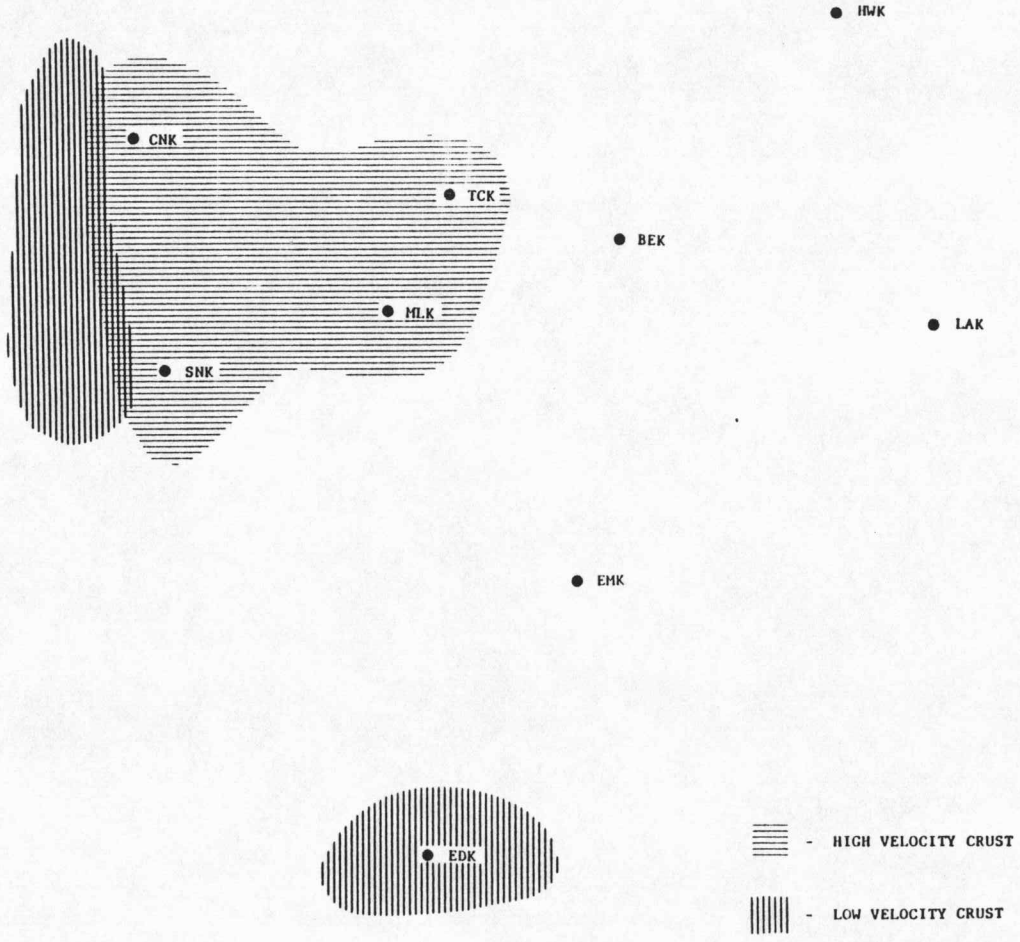

Fig. 13. Pn residuals interpretation.

CONCLUSION

Significant residuals exist to postulate the presence of an anomalously high velocity crustal material in the study area near TCK and MLK (fig 13). Late arrivals at CNK for events from the east and at BEK for events from the west, in association with consistently early arrivals at TCK and MLK, suggest a velocity discontinuity in the crust as well as at the surface of the mantle. This strengthens the results of Hahn (1980), that an anomalous low velocity upper mantle exists below the MGA, and of Lui (1980), that a high velocity crust exists beneath the MGA.

Rock identification of this anomalous material, as well as its approximate column height is not possible with the existing data. From previous studies (Serpa et al., 1983, Bickford et al., 1979), the majority of crustal material in the study area falls within the general classification of granite, with the MGA being composed predominantly of basaltic material.

The crustal model formulated here lacks the precision and therefore, the confidence level associated with most of the conventional reversed refraction profiles conducted in the general area (Steeples, 1976; Stewart, 1968; Tryggvason and Qualls, 1967; Jackson et al., 1965; Stewart et al., 1962). However, sufficient precision is present in the determination of the apparent Pn velocities to make

a significant contribution to the previous repertoire of calculated crustal models. Most of the inaccuracies are the result of either poor calculations of epicentral parameters, improper phase identification, or crustal complexities that cause inconsistent arrivals from event to event.

With proper screening of events, this technique could have great promise for preliminary large scale crustal modeling. It also is a good means of filling the gaps that at present are simply extrapolated between the existing 2-dimensional refraction lines. Consistency in results decreases with increasing complexity of the crust. If epicentral parameters can be determined with greater accuracy, the correlation of phase depths with a smaller window of uncertainty and therefore a more precise model is possible.

A more exact determination of the location and size of the anomalous crustal material, as well as better insight into the rock type that composes this material, can possibly be gained through a more detailed study of events representing epicentral distances less than than Pn crossover.

Some relationship might exist between measured aeromagnetic highs and high velocity crustal material, as well as the correlation of the aeromagnetic low and the

omidirectional velocity delay at EDK. Also of interest would be a study comparing Pn wave delays with the crustal density variation over the network as determined from the Bouguer gravity (Press and Biehler, 1964). Further research using digital correlation techniques should prove useful.

REFERENCES

Bickford, M.E., Harrower, K.L., Nusbaum, R.L., Thomas, J.J., and Nelson, G.E., Preliminary Geologic map of the Precambrian basement rocks of Kansas: Kansas Geological Survey, Lawrence, Kansas, Map M-9, scale 1:500,000, 1979.

Borcherdt, R.D. and Healy, J.H., A method for estimating the uncertainty of seismic velocities measured by refraction techniques: Seism. Soc. Am. Bull., vol. 58, no. 6, pp. 1769-1790, 1968.

Braile, L.W. and Smith, R.B., Guide to the interpretation of crustal refraction profiles: Geophys. J.R. Astr. Soc., vol. 40, pp. 145-176, 1975.

Brown, L., Serpa, L., Setzer, T., Oliver, J., Kaufman, S., Lillie, R., Steiner, D., and Steeples, D., Intra-crustal complexity in the U.S. Mid-continent: Preliminary results from COCORP surveys in N.E. Kansas: Geology, VII, pp. 25-30, 1983.

Byerly, P., The seismic waves from the Port Chicago explosion: Seism. Soc. Am. Bull., vol. 36, no. 4, pp. 331-348, 1946.

Chase, C. and Gilmer, T., Precambrian plate tectonics: The Midcontinent gravity high: Earth and Planetary Sci. Let., vol. 21, pp. 70-78, 1973.

Cole, V.B., Confirguration of the top of the Precambrian rocks in Kansas: Kansas Geological Survey, Lawrence, Kansas, Map M-7, scale 1:500,000, 1976.

Eaton, J.P., Crustal structure in northern and central California from seismic evidence: Geology of Northern California, ed. E.H. Bailey, Cal. Div. Mines Geol. Bull., vol. 190, pp. 419-426, 1966.

Garland, G.D., Introduction to Geophysics: W. B. Saunder Co., 2nd edition, pp. 21-55, 1979.

Hahn, R., Upper mantle velocity structure in eastern Kansas from teleseismic P-wave residuals: Unpublished, M.S. thesis, The University of Kansas, 85 p., 1980.

Herrin, E. and Taggart, J., Regional variations in P_n velocity and their effect on the location of epicenters: Seism. Soc. Am. Bull., vol. 52, no. 5, pp. 1037-1046, 1962.

Hill, D.P., Crustal and upper mantle structure of the Columbia Plateau from long-range seismic-refraction measurements: Geol. Soc. of Am. Bull., vol. 83, pp. 1639-1648, 1972.

Hill, D.P., Structure of Long Valley Caldera, California, from a seismic refraction experiment: J. Geophy. Res., vol. 81, no. 5, pp. 745-753, 1976.

Jackson, W.H. and Pakiser, L.C., Seismic study of crustal structure in the southern Rocky Mountains: U.S. Geol. Survey Prof. Paper 525-D, pp. D85-D92, 1965.

King, E. and Zeitz, I., Aeromagnetic study of the Midcontinent gravity high of the central United States: G.S.A. Bull., vol. 82, pp. 2187-2208, 1971.

Lui, C.Y., Microearthquake in Red Willow County, Nebraska: Unpublished M.S. thesis, The University of Kansas, 53 p., 1980.

Masse, R.P., Compressional velocity distribution beneath central and eastern North America: Seism. Soc. Am. Bull., vol. 63, no. 3, pp. 911-935, 1973.

McCamy, K. and Meyer, R.P., Crustal results of fixed multiple shots in the Mississippi embayment: Am. Geophys. Union, Geophys. Monogr. Ser. 10, pp. 370-381, 1966.

Mintrop, L., On the stratification of the Earth's crust according to seismic studies of a large explosion and of earthquakes: Geophysics, vol. XIV., no. 3, pp. 321-336, 1949.

Mitchell, B.J. and Landisman, M, Geophysical measurements in the southern great plains: In J.G. Heacock (editor), The structure and physical properties of the Earth's crust, Am. Geophys. Union, Geophys. Monogr. Ser. 14, pp. 77-93, 1971.

Mooney, W.D., Crustal and upper mantle velocity structure of central Yunnan Province, Southwest China using earthquake sources: Unpublished, 1982.

Mueller, S., A new model of the continental crust: The Earth's Crust, Am. Geophys. Union, Geophys. Monogr. Ser. 20, pp. 289-317, 1977.

Ocola, L.C. and Meyer, R.P., Central North American Rift System: 1. Structure of the axial zone from seismic and gravimetric data: J. Geophys. Res., vol. 78, pp. 5173-5194, 1973.

Newmann, F., Principals underlying the interpretation of seismograms: Special publication no. 254, Coast and Geodetic Survey, U.S. Dept. of Commerce, 1966.

Pakiser, L.C., Structure of the crust and upper mantle in the western United States: J. Geophys. Res., vol. 68, no. 20, pp. 5747-5756, 1963.

Pakiser, L.C. and Zietz, I., Transcontinental crust and upper-mantle structure: Reviews of Geophysics, vol. 3, no. 4, pp. 505-520, 1965.

Press, F. and Biehler, S., Inferences on crustal velocities and densities from P-wave delays and gravity anomalies: J. Geophys. Res., vol. 69, pp. 2979-2995, 1964.

Richter, C.F., Elementary seismology: W.H. Freeman Co., San Francisco, California, 768 p., 1958.

Serpa, L., Setzer, T., Farmer, H., Brown, L., Oliver, J., Kaufman, S., Sharp, J., and Steeples, D.W., Structure of the southern Keweenawan Rift from COCORP surveys across the Midcontinent Geophysical Anomaly in northeastern Kansas: Submitted to Tectonics, 1983.

Sheehan, A. and Steeples, D.W., Sensitivity of Kansas microearthquake network: In press, Earthquake Notes, 1983.

Snyder, F.G., Tectonic history of midcontinental United States: University of Missouri--Rolla Journal, no. 1, pp. 65-77, 1968.

Steeples, D.W., Preliminary crustal model for northwest Kansas, (Abs.): EOS, 57, 961, 1976.

Steeples, D.W., Microearthquake network in Kansas, terrestrial and space techniques in earthquake prediction research: Friedr. Vieweg & Sohn Braunschweig/Wiesbaden, pp. 115-130, 1978.

Steeples, D.W., Structure of the Salina-Forest City interbasin boundary from seismic studies: University of Missouri--Rolla Journal no. 3, pp. 55-81, 1982.

Steinhart, J.S. and Meyer, R.P., Explosion studies of continental structure: Carnegie Inst., Wash. #622, 409 p., 1961.

Stewart, S.W., Crustal structure in Missouri by seismic refraction methods: Seismol. Soc. Am. Bull. 58, 291-293, 1968.

Stewart, S.W. and Pakiser, L.C., Crustal structure in eastern New Mexico interpreted from the Gnome explosion: Seismol. Soc. Am. Bull. 52, pp. 1017-1030, 1962.

Telford, W.M., Geldart, L.P., Sheriff, R.E., and Kays, D.A., Applied Geophysics, Cambridge University Press, pp. 218-434, 1976.

Tryggvason, E. and Qualls, B.R., Seismic refraction measurements of crustal structure in Oklahoma: J. Geophys. Res., 72, pp. 3738-3740, 1967.

Van Schmus, W.R. and Bickford, M.E., Proterozoic chronology and evolution of the midcontinental region, North America, in Precambrian Plate Tectonics: Edited by A. Kroner, Elsevier, New York, 1982.

Warren, D.H. and Healy, J.H., Structure of the crust in the conterminous United States: Tectonophysics, vol. 20, pp. 203-213, 1973.

Warrick, R.E., Hoover, D.B., Jackson, W.H., Pakiser, L.C., and Roller, J.C., The specifications and testing of a seismic refraction system for crustal studies: Geophysics, vol. 26, pp. 820-824, 1961.

Yarger, H.L., Ng, K., Robertson, R., and Woods, R., Bouguer gravity map of northeastern Kansas: Kansas Geological Survey, Lawrence, Kansas, scale 1:500,000, 1980.

Yarger, H.L., Aeromagnetic Survey of Kansas: EOS Trans., Amer. Geophys. Union, vol. 62, no. 17, pp. 173-178, 1981.

Yarger, H.L., Regional interpretation of Kansas aeromagnetic data: Kansas Geological Survey Geophysics Series, no. 1, 35 p., 1983.

APPENDIX

ARKANSAS

June 9, 1981

Event #1

LAT: 37.825°N

LONG: 89.027°W

ORIGIN TIME: 1415:47.8

M_{bLg}: 3.5

DEPTH: 19.0 km (+3.0 sec)

DIGIT-ORIGIN: 1417:00.0

Station	Epi-Dist	Pn resid	Corrected Pn resid TCK	HWK	EDK	Pn/w	P1/w	P2/w	Pg/w
HWK	602.0	-0.2	+0.2	0.0		83.75/2	87.2/2	90.2/1	100.0/2
EMK	641.3	-0.1	-0.2	0.0		88.15/2	93.7/3	98.15/2	106.8/2
BEK	643.9	-0.2	-0.3	-0.2		88.35/1	94.25/2	98.05/2	107.6/1
TCK	690.8	+0.2	+0.3	+0.2		94.4/2	99.75/1	103.9/2	116.2/2
MLK	699.4	-0.1	-0.3	-0.2		95.1/3	100.45/1	104.55/2	117.85/2

	Pn/w	P1/w	P2/w	Pg/w
VELOCITY (km/sec)	8.38	7.38	6.80	5.41
Y INTERCEPT (km)	-98.4	-49.4	-22.4	-9.6
X INTERCEPT (sec)	11.7	6.7	3.3	-
CORRELATION	0.999	0.993	0.986	0.999
LAYER DEPTH (km)	64.6	40.9	14.7	-

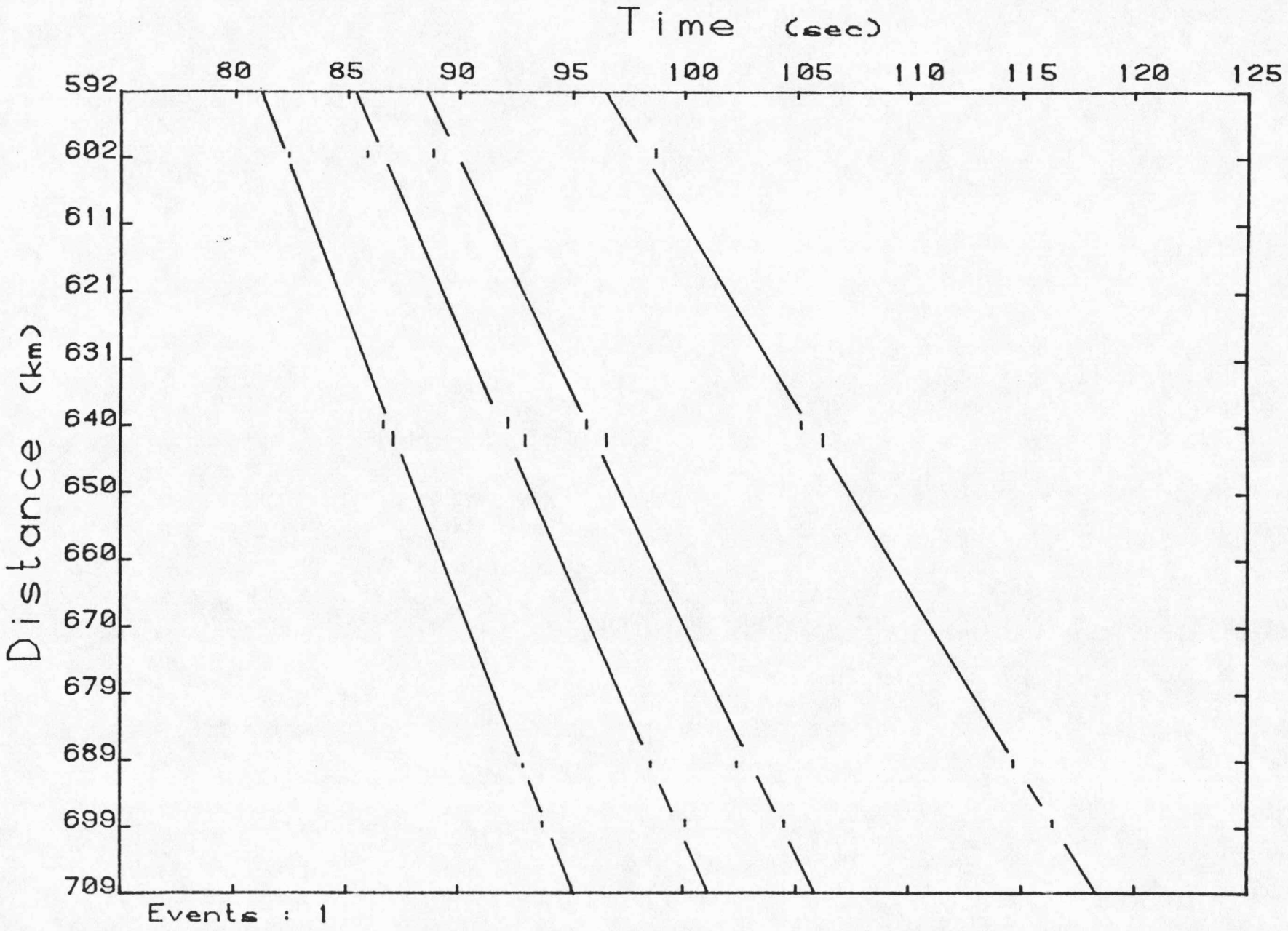
Time (sec)
80
85
90
95
100
105
110
115
120
125
Distance (km)
592
602
611
621
631
640
650
660
670
679
689
699
709
Events : 1

ARKANSAS

January 21, 1982

Event #2

LAT: 35.180°N

LONG: 92.250°W

ORIGIN TIME: 0033:54.2

M_{bLg}: 4.5

DEPTH: 4.1 km (+1.0 sec)

DIGIT-ORIGIN: 0035:00.0

Station	Epi-Dist	Pn resid	Corrected Pn resid TCK	HWK	EDK	Pn/w	Pl/w	P2/w	Pg/w
EDK	498.2	+0.7	+0.7	+0.8	+0.5	71.1/3	73.05/3	76.05/3	81.25/3
EMK	512.8	-0.2	-0.3	-0.2	-0.2	71.9/2	75.0/2	78.05/2	83.35/2
BEK	573.0	-0.5	-0.5	-0.5	-0.4	79.0/2	82.2/1	85.4/3	93.2/3
HWK	588.3	+0.6	+0.7	+0.4	+0.7	82.0/2	85.3/2	88.7/2	97.45/2
MLK	599.7	-0.6	-0.6	-0.6	-0.5	82.15/3	86.75/3	89.35/3	98.0/3
TCK	612.3	-0.7	-0.3	-0.6	-0.8	83.65/3	88.1/2	91.15/2	99.2/2
SNK	633.5	-0.3	-0.2	-0.2	-0.2	86.6/2	90.95/1	94.8/2	103.9/2
CNK	681.5	+0.6	+0.6	+0.6	+0.6	93.3/2	97.75/2	103.4/2	113.85/1
NRTK	862.8	-0.1	0.0	0.0	-0.1	114.7/1	120.45/2	127.4/3	141.4/2

VELOCITY (km/sec)	8.22	7.65	7.00	6.00
Y INTERCEPT (km)	-79.9	-62.3	-30.9	10.3
X INTERCEPT (sec)	9.7	8.1	4.4	-
CORRELATION	0.999	1.000	0.999	0.999
LAYER DEPTH (km)	52.2	49.9	25.6	

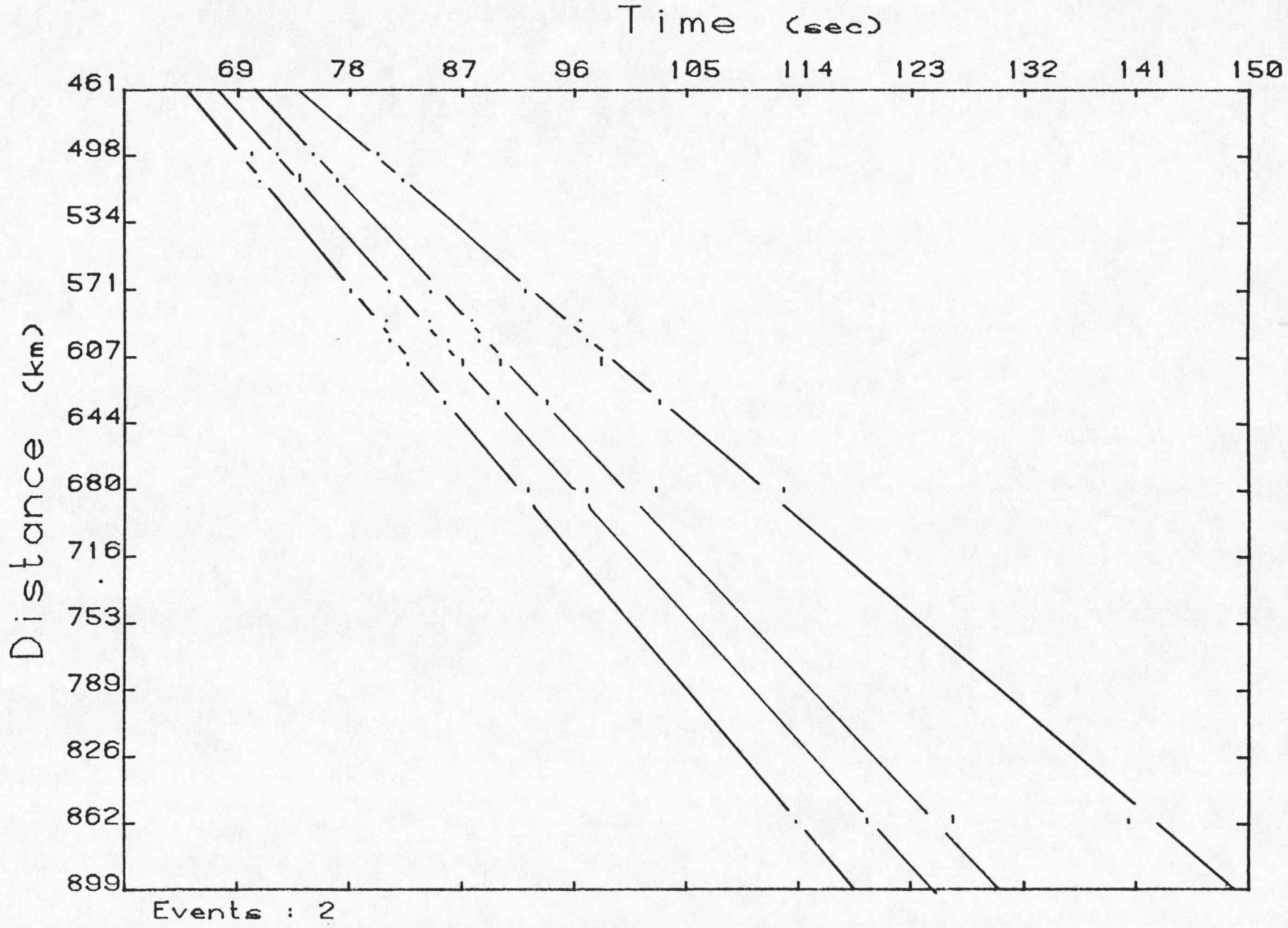
Time (sec)
69
78
87
96
105
114
123
132
141
150
Distance (km)
461
498
534
571
607
644
680
716
753
789
826
862
899
Events : 2

ARKANSAS

January 22, 1982

Event #3

LAT: 35.247°N

LONG: 92.290°W

ORIGIN TIME: 2354:22.6

M_{bLg}: 3.7

DEPTH: 3.0 (+0.5 sec)

DIGIT-ORIGIN: 2355:20.0

Station	Epi-Dist	Pn resid	Corrected Pn resid TCK	HWK	EDK	Pn/w	P1/w	P2/w	Pg/w
EDK	490.9	+0.2	+0.2		0.0	70.05/3	71.7/3	75.3/3	79.9/2
EMK	504.9	+0.3	+0.2		+0.3	71.8/1	73.8/2	77.7/2	82.9/2
BEK	564.8	-0.2	-0.3		-0.2	78.7/2	81.55/2	85.2/2	92.6/3
MLK	591.8	+0.5	+0.5		+0.6	82.75/2	86.1/3	89.65/3	97.6/3
TCK	604.3	-0.5	-0.3		-0.6	83.2/2	86.85/3	90.6/2	98.95/2
SNK	625.8	-0.4	-0.5		-0.4	86.0/2	89.7/2	94.1/2	103.6/2
NRTK	855.3	+0.3	+0.2		+0.1	114.8/2	-	-	-
					VELOCITY (km/sec)	8.14	7.43	7.30	5.83
					Y INTERCEPT (km)	-77.4	-42.6	-59.6	22.6
					X INTERCEPT (sec)	9.5	5.7	8.2	-
					CORRELATION	1.000	0.999	0.999	0.999
					LAYER DEPTH (km)	45.2	-14.1	39.7	-

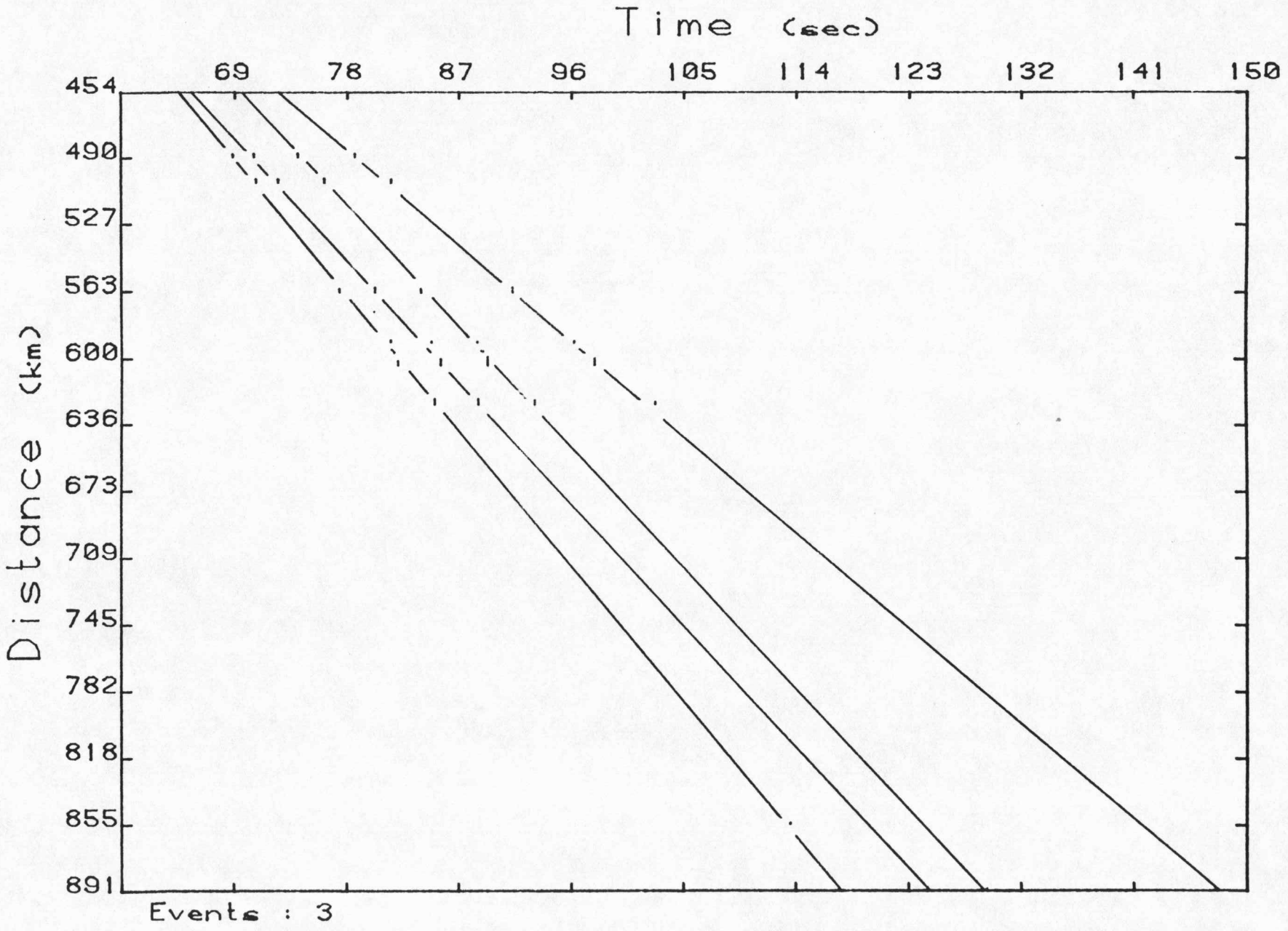
Time (sec)
69
78
87
96
105
114
123
132
141
150
Distance (km)
454
490
527
563
600
636
673
709
745
782
818
855
891
Events : 3

ARKANSAS

January 24, 1982

Event #4

LAT: 35.210°N

LONG: 92.180°W

ORIGIN TIME: 0322:45.1

M_{bLg}: 4.2

DEPTH: 5.3 km (+1.0 sec)

DIGIT-ORIGIN: 0323:50.0

Station	Epi-Dist	Pn resid	Corrected Pn resid TCK	HWK	EDK	Pn/w	P1/w	P2/w	Pg/w
EDK	501.4	+0.2	+0.1		0.0	70.2/1	72.0/2	74.75/2	80.25/2
EMK	514.8	+0.1	+0.1		+0.2	71.75/1	74.5/1	77.65/2	82.45/2
BEK	574.1	0.0	-0.1		0.0	78.8/1	81.75/1	85.4/2	93.05/2
MLK	601.6	-0.4	-0.4		-0.3	81.8/3	85.8/2	88.7/2	98.25/3
TCK	613.8	+0.1	+0.3		0.0	83.65/1	87.8/2	91.45/2	101.4/2
SNK	635.9	-0.1	-0.2		-0.1	86.2/1	90.55/3	93.05/2	104.45/2
CNK	683.5	+0.1	+0.2		+0.2	92.3/2	97.2/3	102.65/3	114.4/3
NRTK	865.6	-	-		-	114.45/4	120.7/2	126.55/2	144.8/3
			VELOCITY (km/sec)			8.28	7.50	7.02	5.59
			Y INTERCEPT (km)			-78.8	-41.7	-25.3	-
			X INTERCEPT (sec)			9.5	5.6	3.6	-
			CORRELATION			1.000	1.000	0.999	0.999
			LAYER DEPTH (km)			53.4	32.9	16.6	-

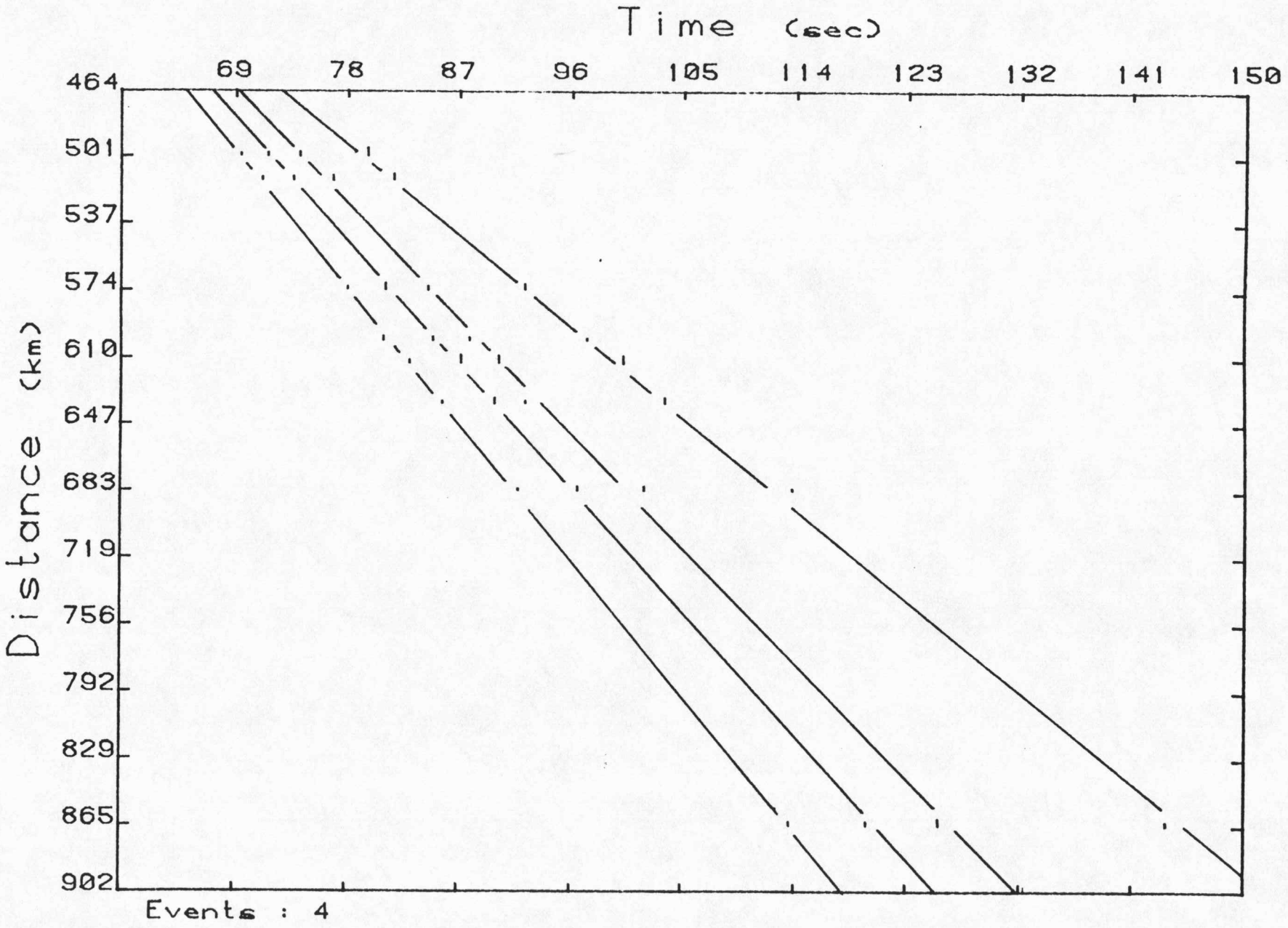
Time (sec)
69
78
87
96
105
114
123
132
141
150
Distance (km)
464
501
537
574
610
647
683
719
756
792
829
865
902
Events : 4

ILLINOIS

April 8, 1981

Event #5

LAT: 35.868°N

LONG: 89.386°W

ORIGIN TIME: 0153:13.2

M_{bLg}: 3.8

DEPTH: 7 km (+1.0 sec)

DIGIT-ORIGIN: 0154:20.0

Station	Epi-Dist	Pn resid	Corrected Pn resid TCK	HWK	EDK	Pn/w	P1/w	P2/w	Pg/w
HWK	535.7	0.0	-0.1	-0.1		74.35/1	77.1/2	80.05/1	86.85/2
BEK	589.9	+0.3	+0.2	+0.4		81.5/1	85.35/2	88.7/2	96.05/2
EMK	603.7	+0.2	+0.1	+0.3		83.2/1	87.2/2	90.9/3	98.65/2
TCK	635.4	-0.5	-0.2	-0.4		86.55/1	90.85/3	94.7/3	103.25/2
MLK	649.3	-0.4	-0.4	-0.3		88.4/2	92.95/2	96.9/3	105.9/2
SNK	711.0	+0.2	+0.2	+0.2		96.85/2	102.3/2	106.5/2	117.0/2
CNK	721.2	0.0	-0.1	0.0		97.9/2	103.5/2	107.8/3	118.95/2
		VELOCITY (km/sec)				7.88	7.06	6.73	5.8
		Y INTERCEPT (km)				-50.2	-9.5	-3.9	-
		X INTERCEPT (sec)				6.4	1.3	0.5	-
		CORRELATION				0.999	0.999	0.999	0.999
		LAYER DEPTH (km)				46.5	11.0	2.9	-

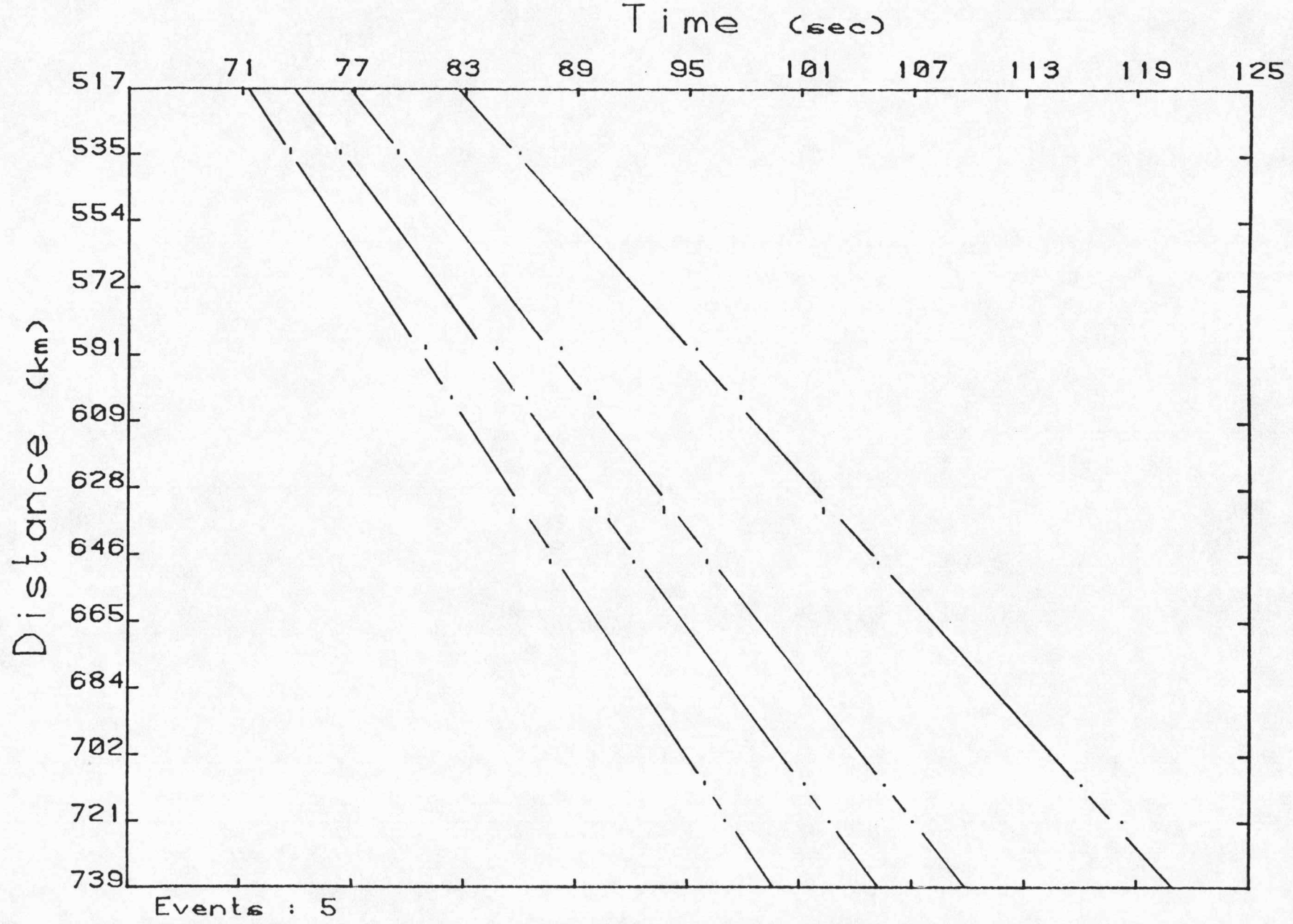
Time (sec)
71
77
83
89
95
101
107
113
119
125
Distance (km)
517
535
554
572
591
609
628
646
665
684
702
721
739
Events : 5

KENTUCKY

July 27, 1980

Event #6

LAT: 38.190°N

LONG: 83.950°W

ORIGIN TIME: 1852:21.6

M_{bLg}: 5.0

DEPTH: 10.0 km (+2.0 sec)

DIGIT-ORIGIN: 1854:20.0

Station	Epi-Dist	Pn resid	Pn/w
LAK	982.0	-	130.1/4
HWK	1013.7	-0.4	132.85/1
BEK	1069.3	-0.2	139.3/2
EMK	1079.3	-0.4	140.2/2
TCK	1114.9	+0.3	145.0/1
EDK	1126.7	-	147.0/4
MLK	1128.5	+0.4	146.6/1
CNK	1200.8	0.0	154.4/1
GOL	1860.5	-0.2	228.5/1

VELOCITY (km/sec)	8.87
Y INTERCEPT (km)	-168.4
X INTERCEPT (sec)	19.0
CORRELATION	1.000

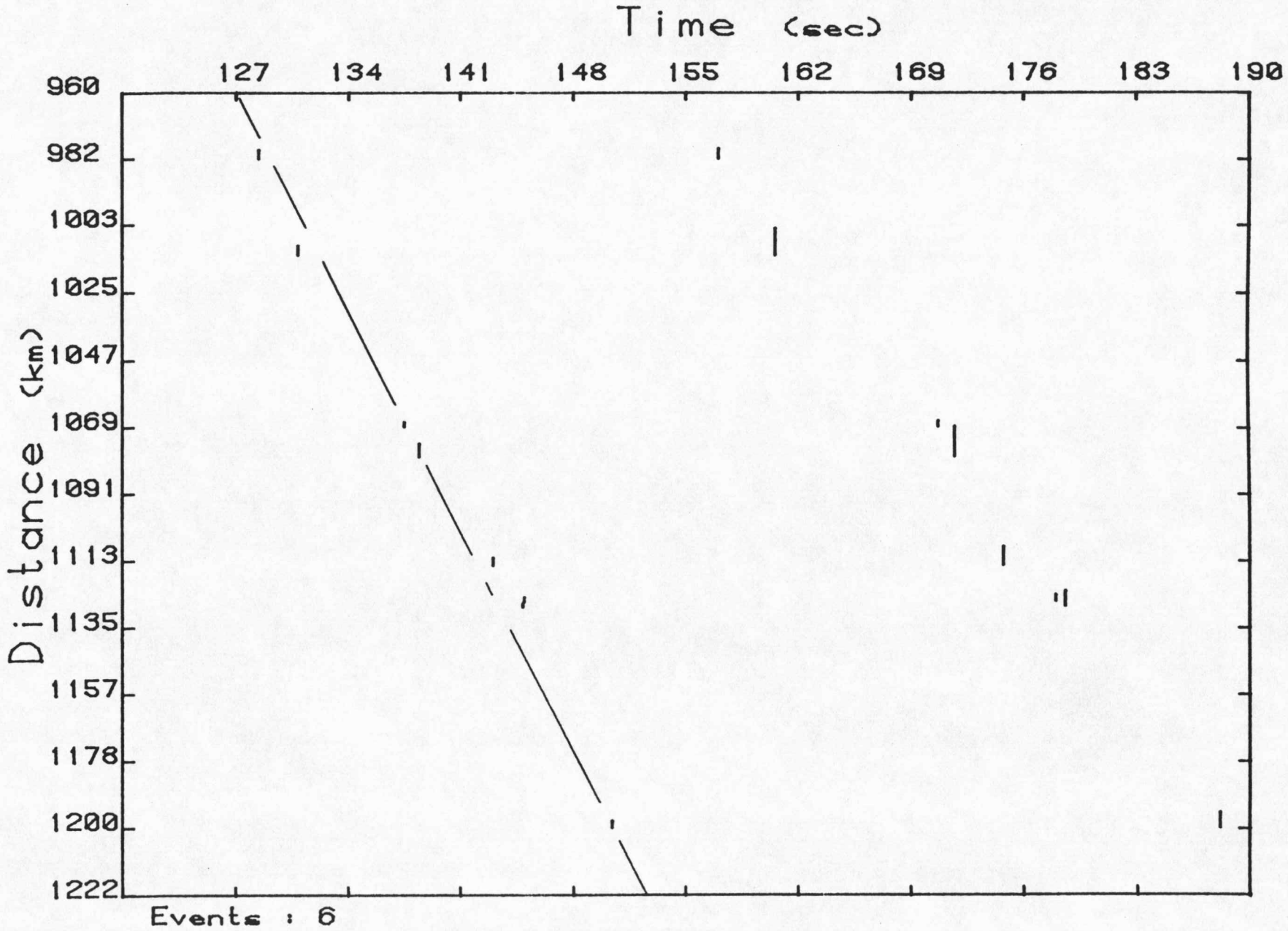
Time (sec)
127
134
141
148
155
162
169
176
183
190
Distance (km)
960
982
1003
1025
1047
1069
1091
1113
1135
1157
1178
1200
1222
Events : 6

TENNESSEE

December 2, 1980

Event #7

LAT: 36.210°N

LONG: 89.430°W

ORIGIN TIME: 0859:30.0

M_{bLg}: 3.8

DEPTH: 10.7 km (+1.5 sec)

DIGIT-ORIGIN: 0900:40.0

Station	Epi-Dist	Pn resid	Corrected Pn resid TCK	HWK	EDK	Pn/w	Pl/w	P2/w	Pg/w
LAK	598.3	0.0	0.0	0.0		82.1/2	85.5/1	89.15/1	97.4/3
EMK	657.7	+0.3	+0.3	+0.3		89.75/2	94.15/1	98.5/2	107.5/2
HWK	664.7	+0.1	0.0	+0.2		90.4/1	-	99.3/2	107.85/3
BEK	685.1	0.0	0.0	0.0		92.85/1	98.5/2	102.1/3	112.8/2
TCK	731.3	-0.5	-0.3	-0.6		98.0/1	103.05/2	107.0/2	118.0/3
MLK	731.4	-0.1	-0.3	-0.2		98.4/2	103.25/2	107.5/2	118.4/2
SNK	781.9	+0.4	+0.3	+0.4		105.2/2	111.15/1	116.25/2	129.95/3
VELOCITY (km/sec)						8.09	7.34	7.04	5.80
Y INTERCEPT (km)						-65.9	-30.8	-30.7	-
X INTERCEPT (sec)						8.1	4.2	4.4	-
CORRELATION						0.999	0.997	0.996	0.993
LAYER DEPTH (km)						47.5	15.6	22.5	-

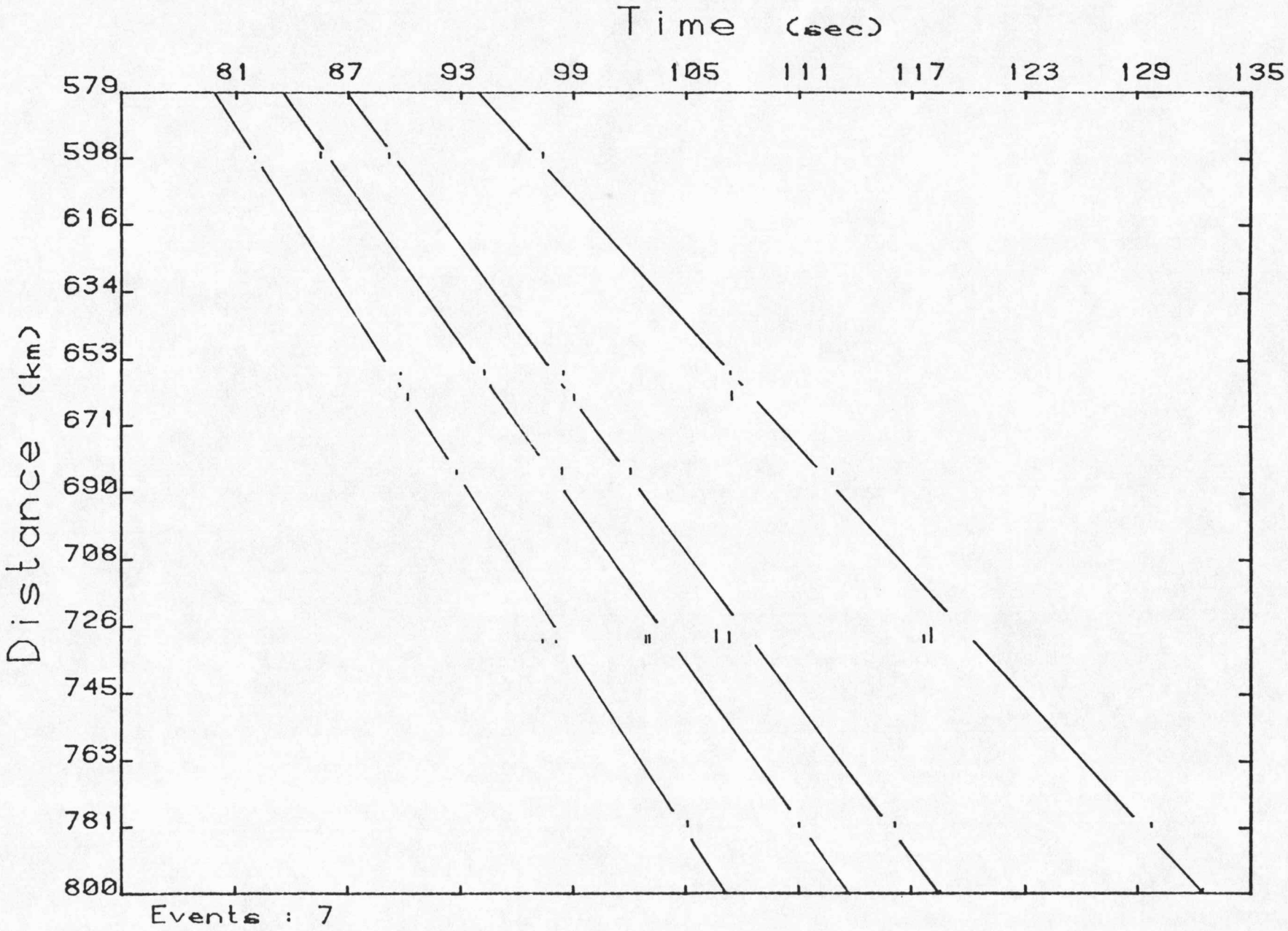
Time (sec)
81
87
93
99
105
111
117
123
129
135
Distance (km)
579
598
616
634
653
671
690
708
726
745
763
781
800
Events : 7

OKLAHOMA

June 7, 1979

Event #8

LAT: 35.187°N

LONG: 99.812°W

ORIGIN TIME: 0739:35.6

M_{bLg}: 3.0

DEPTH: 5.0 km (+1.0 sec)

DIGIT-ORIGIN: 0740:30.0

Station	Epi-Dist	Pn resid	Corrected Pn resid TCK	HWK	EDK	Pn/w	Pl/w	P2/w	Pg/w
EDK	394.3	+0.7	+0.6	+0.6	+0.5	57.6/2	59.9/3	61.55/2	64.95/1
SNK	462.3	-1.3	-1.3	-1.3	-1.2	63.8/1	66.1/3	68.25/3	73.65/2
EMK	477.6	+1.0	+0.9	+1.0	+1.0	67.9/3	71.25/2	73.8/2	78.7/3
MLK	506.7	-0.5	-0.6	-0.5	-0.5	69.9/1	73.8/3	76.8/2	81.5/1
TCK	540.8	0.0	+0.2	-0.1	0.0	74.5/2	78.85/2	86.0/1	86.75/2
HWK	638.8	-0.2	0.0	0.0	0.0	86.4/1	91.4/3	96.5/0	102.65/1

	Pn/w	Pl/w	P2/w	Pg/w
VELOCITY (km/sec)	8.34	7.53	6.79	6.40
Y INTERCEPT (km)	-80.3	-50.3	-16.2	-15.2
X INTERCEPT (sec)	9.6	6.7	2.4	2.4
CORRELATION	0.997	0.995	0.995	0.999
LAYER DEPTH (km)	55.3	45.9	23.0	-

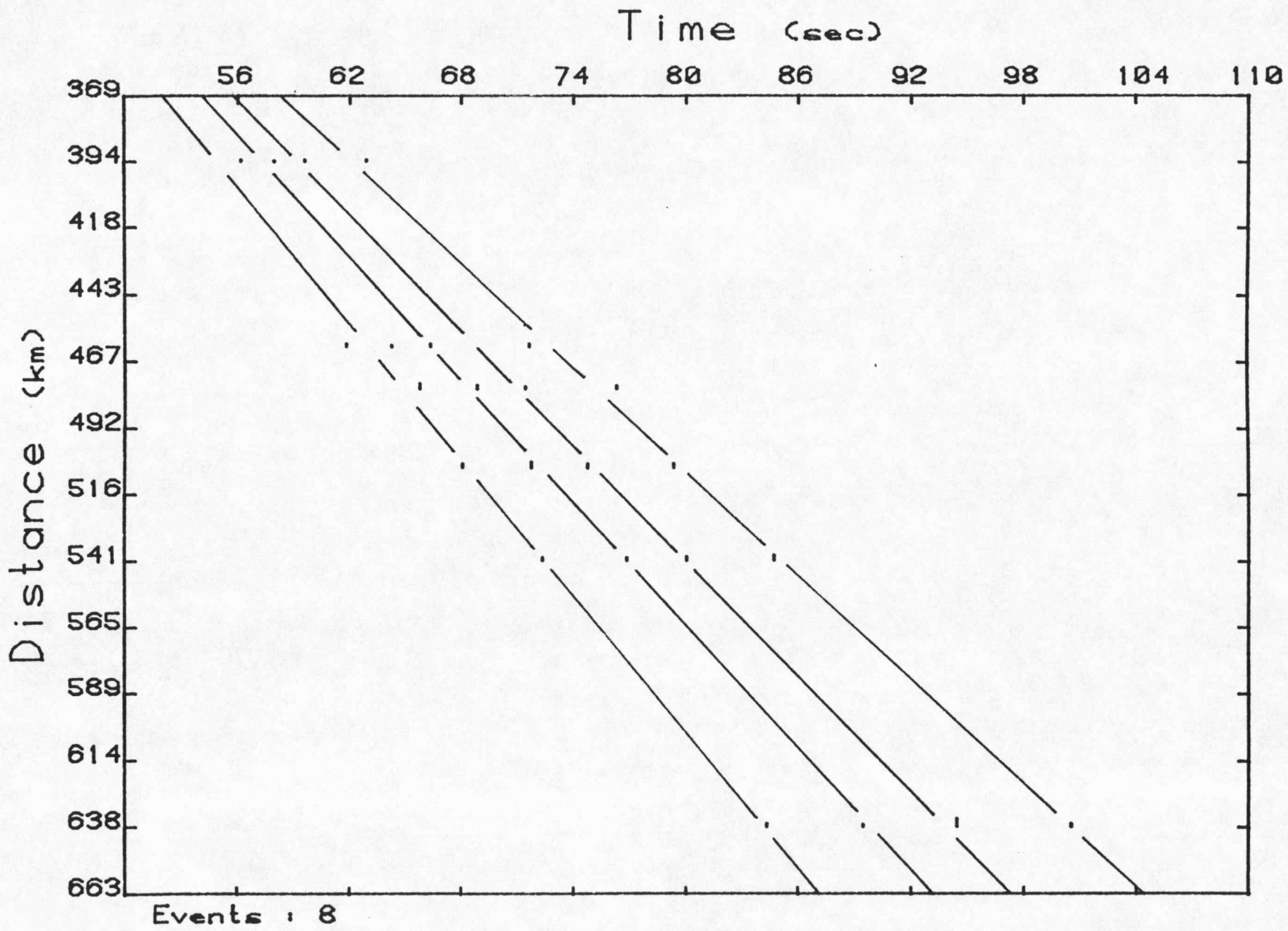
Time (sec)
56
62
68
74
80
86
92
98
104
110
Distance (km)
369
394
418
443
467
492
516
541
565
589
614
638
663
Events : 8

OKLAHOMA

September 13, 1979

Event #9

LAT: 35.217°N

LONG: 99.362°W

ORIGIN TIME: 0049:23.0

M_{bLg}: 3.4

DEPTH: 14.5 km (+2.0 sec)

DIGIT-ORIGIN: 0050:10.0

Station	Epi-Dist	Pn resid	Corrected Pn resid TCK	HWK	EDK	Pn/w	P1/w	P2/w	Pg/w
EDK	365.3	+0.4		+0.3	+0.3	54.35/1	56.8/2	58.35/2	63.35/1
SNK	443.7	-1.1		-1.2	-1.0	62.2/3	65.55/3	67.25/3	74.25/4
EMK	449.8	+0.7		+0.6	+0.7	64.7/1	68.25/2	70.55/2	77.1/2
CNK	498.9	-0.3		-0.3	-0.2	69.65/1	74.15/3	77.15/2	83.9/2
BEK	529.8	+0.2		+0.3	+0.3	73.9/2	78.6/2	82.85/1	89.5/3
LAK	563.0	+0.8		+0.8	+0.7	78.35/1	83.5/2	87.3/1	94.8/1
HWK	613.2	-0.4		-0.7	-0.5	83.15/1	89.65/1	94.5/2	102.8/2
VELOCITY (km/sec)						8.35	7.38	6.64	6.21
Y INTERCEPT (km)						-85.3	-49.6	-15.7	-24.9
X INTERCEPT (sec)						10.2	6.7	2.46	-
CORRELATION						0.998	0.998	0.997	0.999
LAYER DEPTH (km)						55.6	44.2	21.1	-

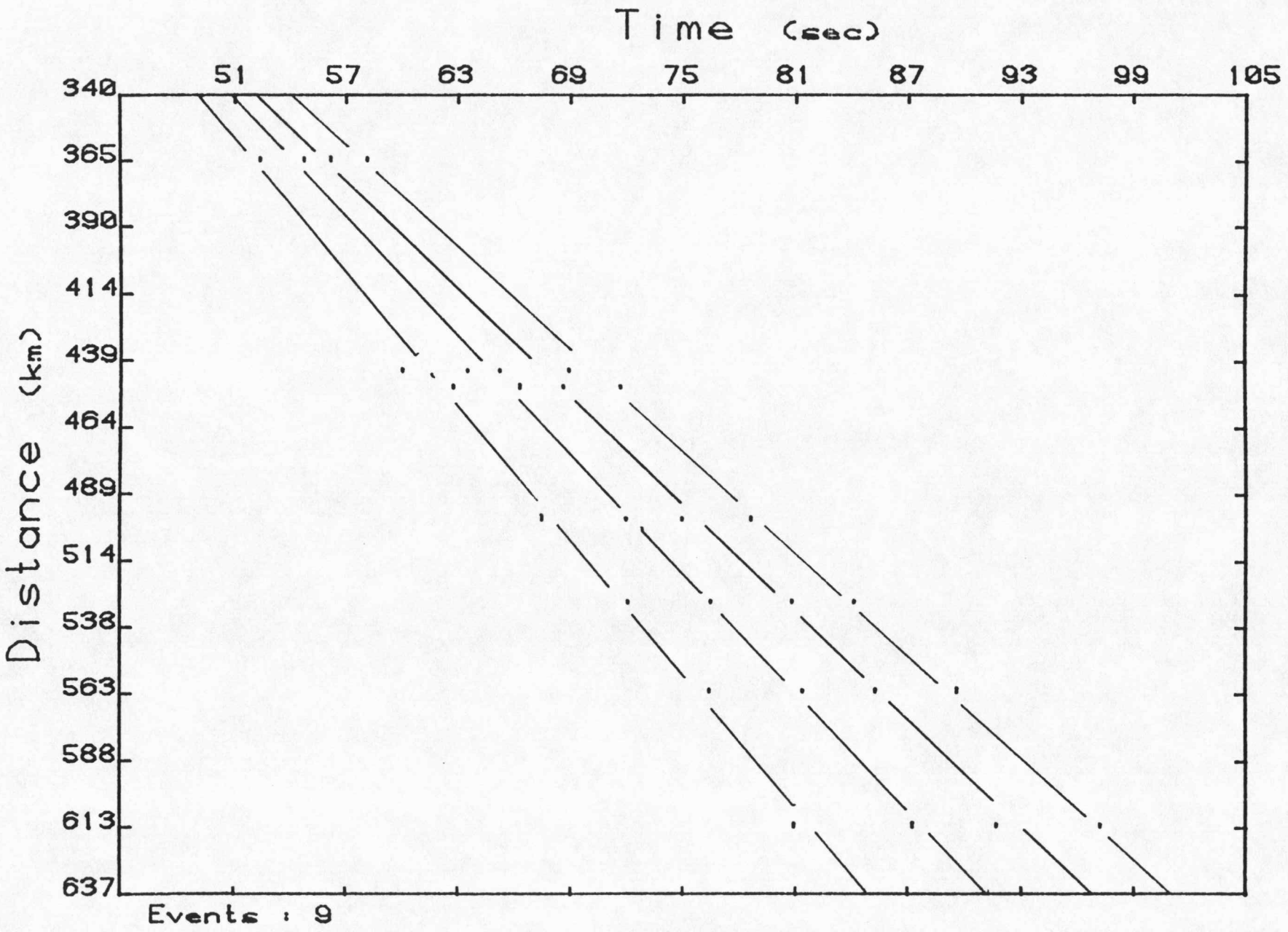
Time (sec)
51
57
63
69
75
81
87
93
99
105
Distance (km)
340
365
390
414
439
464
489
514
538
563
588
613
637
Events : 9

TEXAS

October 14, 1982

Event #10

LAT: 35.999°N

LONG: 102.596°W

ORIGIN TIME: 1252:45.4

M_{bLg}: 3.9

DEPTH: 5 km (+1.0 sec)

DIGIT-ORIGIN: 1254:00.0

Station	Epi-Dist	Pn resid	Corrected Pn resid TCK	HWK	EDK	Pn/w	Pl/w	P2/w	Pg/w
SNK	549.5	+0.3	+0.3	+0.3	+0.5	77.9/1	81.3/2	85.3/3	90.2/2
EDK	552.3	+0.2	+0.2	+0.1	0.0	78.1/1	81.5/2	85.8/2	90.6/2
CNK	580.0	-0.1	-0.1	-0.1	0.0	81.4/2	84.9/3	88.8/2	94.2/3
MLK	610.0	-0.5	-0.5	-0.5	-0.4	84.8/2	89.6/3	93.3/2	98.9/1
EMK	618.9	-0.4	-0.5	-0.3	-0.4	86.1/2	91.6/2	96.6/2	101.2/3
TCK	639.2	-0.4	-0.1	-0.3	-0.3	88.7/3	94.1/3	98.7/3	104.3/2
BEK	669.9	+0.2	+0.2	+0.3	+0.3	93.2/3	99.3/3	104.7/2	110.2/2
LAK	734.5	+0.1	+0.1	+0.3	+0.2	101.4/2	109.1/2	114.0/3	122.7/2
HWK	752.6	0.0	-0.1	-0.2	0.0	103.5/1	111.0/2	116.7/2	124.0/3
VELOCITY (km/sec)						7.81	6.66	6.33	5.77
Y INTERCEPT (km)						-56.3	10.9	12.4	34.0
X INTERCEPT (sec)						7.2	-	-	-
CORRELATION						1.000	0.999	0.998	0.998
LAYER DEPTH (km)						45.9	-	-	-

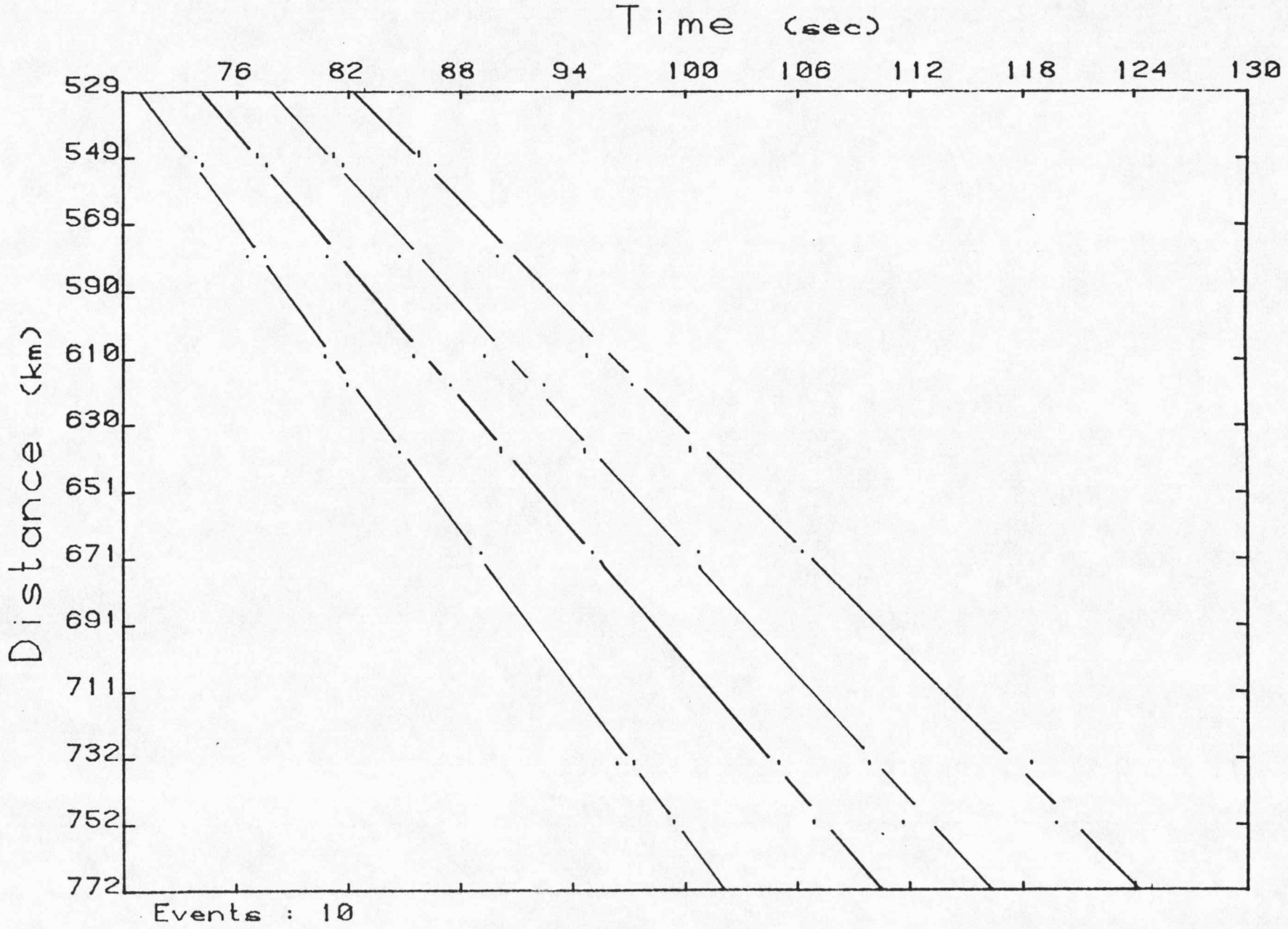
Time (sec)
76
82
88
94
100
106
112
118
124
130
Distance (km)
529
549
569
590
610
630
651
671
691
711
732
752
772
Events : 10

TEXAS

June 16, 1978

Event #11

LAT: 32.961°N

LONG: 100.794°W

ORIGIN TIME: 1146:56.3

M_{bLg}: 4.6

DEPTH: 5.0 km (+1.0 sec)

DIGIT-ORIGIN: 1148:10.0

Station	Epi-Dist	Pn resid	Corrected Pn resid TCK	HWK	EDK	Pn/w	P1/w	P2/w	Pg/w
EDK	646.3	+0.2	+0.1	+0.1	+0.1	87.2/2	91.9/2	95.25/1	102.15/1
SNK	725.4	-0.2	-0.2	-0.1	-0.1	96.7/2	102.65/2	107.8/1	115.85/2
EMK	731.5	+0.5	+0.5	+0.5	+0.6	98.1/2	104.35/1	110.05/2	118.2/2
MLK	767.9	-0.2	-0.3	-0.2	-0.2	101.8/1	108.4/2	114.5/3	123.15/3
CNK	778.5	0.0	0.0	+0.1	+0.1	103.35/2	109.25/2	114.75/2	123.65/2
TCK	802.1	+0.1	+0.3	+0.2	+0.1	106.25/2	113.2/3	119.7/1	128.6/2
BEK	813.0	-0.2	-0.3	-0.2	-0.3	107.2/1	114.7/2	121.25/2	130.1/2
LAK	842.6	+0.5	+0.4	+0.6	+0.5	111.55/2	119.5/2	125.9/3	135.3/2
HWK	896.0	-0.1	-0.3	-0.4	-0.3	117.3/1	125.4/1	131.65/2	141.75/2

	Pn/w	P1/w	P2/w	Pg/w
VELOCITY (km/sec)	8.30	7.42	6.75	6.23
Y INTERCEPT (km)	-78.9	-37.7	-3.7	-
X INTERCEPT (sec)	9.5	5.1	0.5	-
CORRELATION	0.999	0.998	0.996	0.997
LAYER DEPTH (km)	60.3	39.8	4.0	-

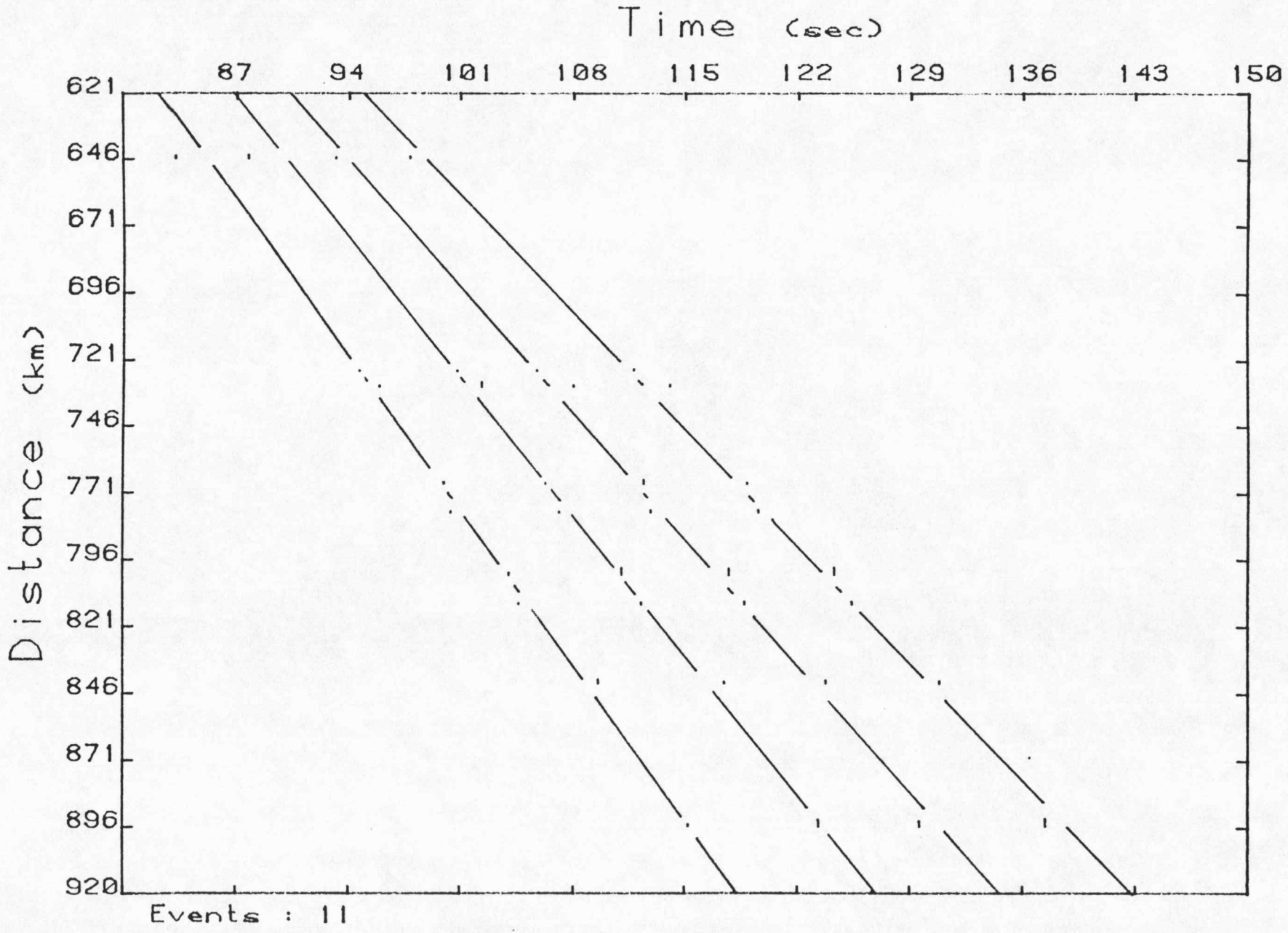
Time (sec)
87
94
101
108
115
122
129
136
143
150
Distance (km)
621
646
671
696
721
746
771
796
821
846
871
896
920
Events : 11

TEXAS

June 9, 1980

Event #12

LAT: 35.476°N

LONG: 100.998°W

ORIGIN TIME: 2237:12.3

M_{bLg}: 3.4

DEPTH: 5.0 km (+1.0 sec)

DIGIT-ORIGIN: 2238:10.0

Station	Epi-Dist	Pn resid	Corrected Pn resid TCK	HWK	EDK	Pn/w	P1/w	P2/w	Pg/w
EDK	453.8	+0.3	+0.2	+0.4	0.0	64.05/1	67.05/2	69.8/3	73.0/1
SNK	489.7	-0.4	-0.5	-0.3	-0.3	67.75/1	71.05/1	74.15/2	77.95/2
EMK	531.0	+0.6	+0.6	+0.8	+0.5	73.85/1	77.7/2	81.0/3	86.45/2
CNK	533.8	-1.0	-1.0	-0.9	-1.0	72.55/1	76.35/1	-	83.8/2
MLK	542.9	+0.8	+0.8	+1.0	+0.6	75.45/1	78.85/2	82.95/1	87.3/2
TCK	575.6	+0.1	+0.3	+0.4	+0.1	78.85/2	83.35/3	87.5/3	92.95/3
BEK	597.4	+0.2	+0.2	+0.5	+0.2	81.6/1	86.2/2	90.7/2	96.3/3
HWK	682.5	-0.3	-0.3	-0.2	-0.4	91.45/2	-	-	-
VELOCITY (km/sec)						8.19	7.33	6.73	6.01
Y INTERCEPT (km)						-68.8	-35.0	-15.3	-
X INTERCEPT (sec)						8.4	4.8	2.3	-
CORRELATION						0.998	0.994	0.999	0.996
LAYER DEPTH (km)						49.6	31.3	15.4	-

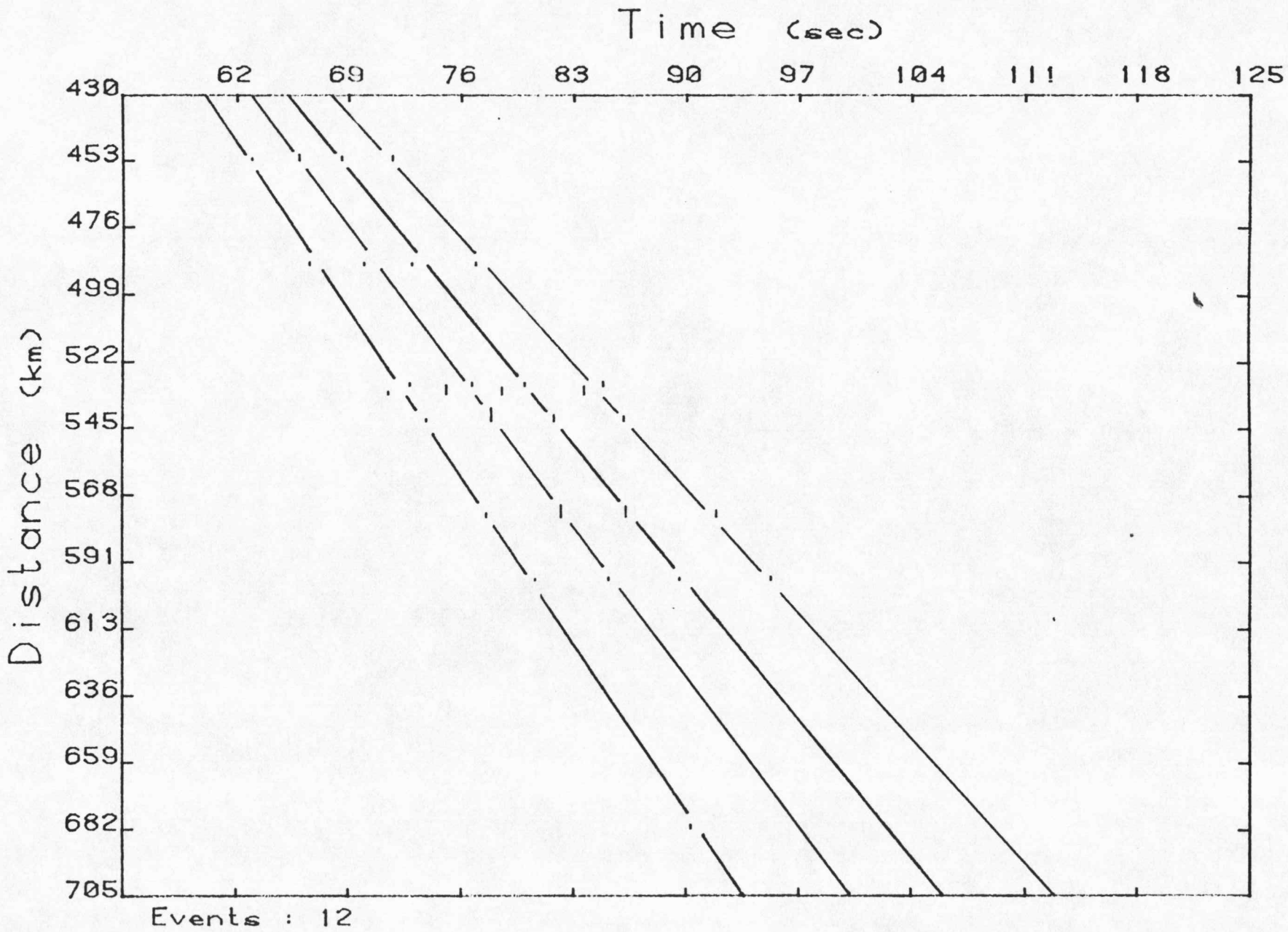
Time (sec)
62
69
76
83
90
97
104
111
118
125
Distance (km)
430
453
476
499
522
545
568
591
613
636
659
682
705
Events : 12

MINNESOTA

July 11, 1982

Event #13

LAT: 43.925°N

LONG: 96.740°W

ORIGIN TIME: 1942:28.4

M_{bLg}: 3.6

DEPTH: 5 km (+1.0 sec)

DIGIT-ORIGIN: 1943:30.0

Station	Epi-Dist	Pn resid	Corrected Pn resid TCK	HWK	EDK	Pn/w	P1/w	P2/w	Pg/w
HWK	469.8	+0.9	+0.8	+0.7	+0.8	71.85/3	75.1/2	78.35/3	81.6/2
CNK	497.8	-0.5	-0.6	-0.5	-0.6	73.7/3	77.7/2	81.55/1	84.8/1
TCK	504.8	-0.1	-0.1	0.0	-0.2	75.0/2	79.45/3	82.95/2	87.1/3
BEK	520.3	0.0	0.0	+0.1	0.0	76.95/3	81.45/3	85.9/3	89.05/3
MLK	536.0	0.0	-0.1	0.0	-0.1	78.75/3	-	-	91.55/3
LAK	557.3	0.0	+0.1	+0.2	+0.2	81.5/2	86.35/2	90.7/3	95.1/3
SNK	557.5	-0.5	-0.6	-0.5	-0.6	80.8/1	86.25/2	90.0/1	94.35/3
EMK	610.2	0.0	+0.1	0.0	0.0	87.55/2	93.95/2	97.5/2	102.95/2
EDK	684.0	+0.3	+0.2	+0.3	+0.1	96.7/1	104.0/2	108.1/2	115.85/2

	Pn/w	P1/w	P2/w	Pg/w
VELOCITY (km/sec)	8.40	7.29	7.17	6.21
Y INTERCEPT (km)	-125.7	-72.9	-91.1	-
X INTERCEPT (sec)	15.0	10.0	12.7	-
CORRELATION	0.998	0.999	0.999	0.999
LAYER DEPTH (km)	67.8	13.3	-	-

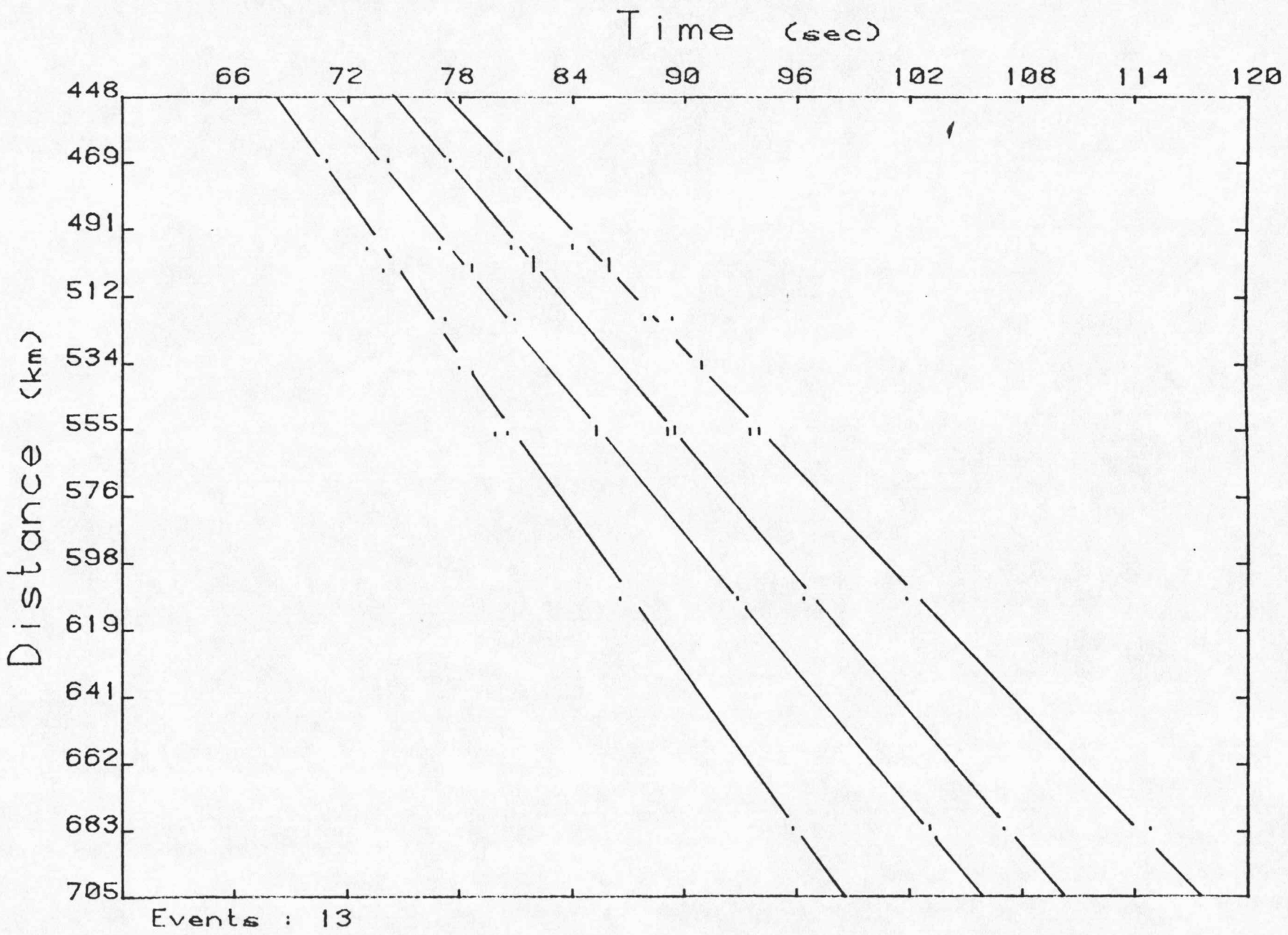
Time (sec)
66
72
78
84
90
96
102
108
114
120
Distance (km)
448
469
491
512
534
555
576
598
619
641
662
683
705
Events : 13

SOUTH DAKOTA

November 15, 1982

Event #14

LAT: 43.149°N

LONG: 97.739°W

ORIGIN TIME: 0258:18.2

M_{bLg}: 4.3

DEPTH: 5 km (+1.0 sec)

DIGIT-ORIGIN: 0259:10.0

Station	Epi-Dist	Pn resid	Corrected Pn resid TCK	HWK	EDK	Pn/w	P1/w	P2/w	Pg/w
CNK	404.9	-0.1	-0.2	0.0	-0.1	60.7/1	63.1/2	65.75/3	68.4/2
HWK	416.4	+0.3	+0.3	+0.2	+0.4	62.55/1	65.1/2	67.8/2	71.3/2
TCK	427.1	-0.3	0.0	-0.2	-0.3	63.2/1	65.95/2	68.55/2	72.15/3
BEK	450.8	+0.1	+0.1	+0.2	+0.2	66.45/1	69.75/3	73.05/3	76.4/2
SNK	466.7	-0.4	-0.4	-0.4	-0.3	67.8/1	71.3/2	74.7/3	79.05/2
LAK	503.2	+0.4	+0.4	+0.5	+0.5	73.0/1	77.5/2	80.9/3	84.95/3
EMK	536.4	-0.3	-0.3	-0.2	-0.1	76.25/1	81.2/2	85.2/3	89.25/3
EDK	603.0	0.0	+0.1	0.0	-0.1	84.5	90.9/2	94.4/2	100.3/3

	Pn/w	P1/w	P2/w	Pg/w
VELOCITY (km/sec)	8.36	7.14	6.86	6.28
Y INTERCEPT (km)	-103.6	-45.2	-47.4	-30.2
X INTERCEPT (sec)	12.4	6.3	6.9	-
CORRELATION	0.999	0.999	0.999	0.999
LAYER DEPTH (km)	64.6	30.9	-	-

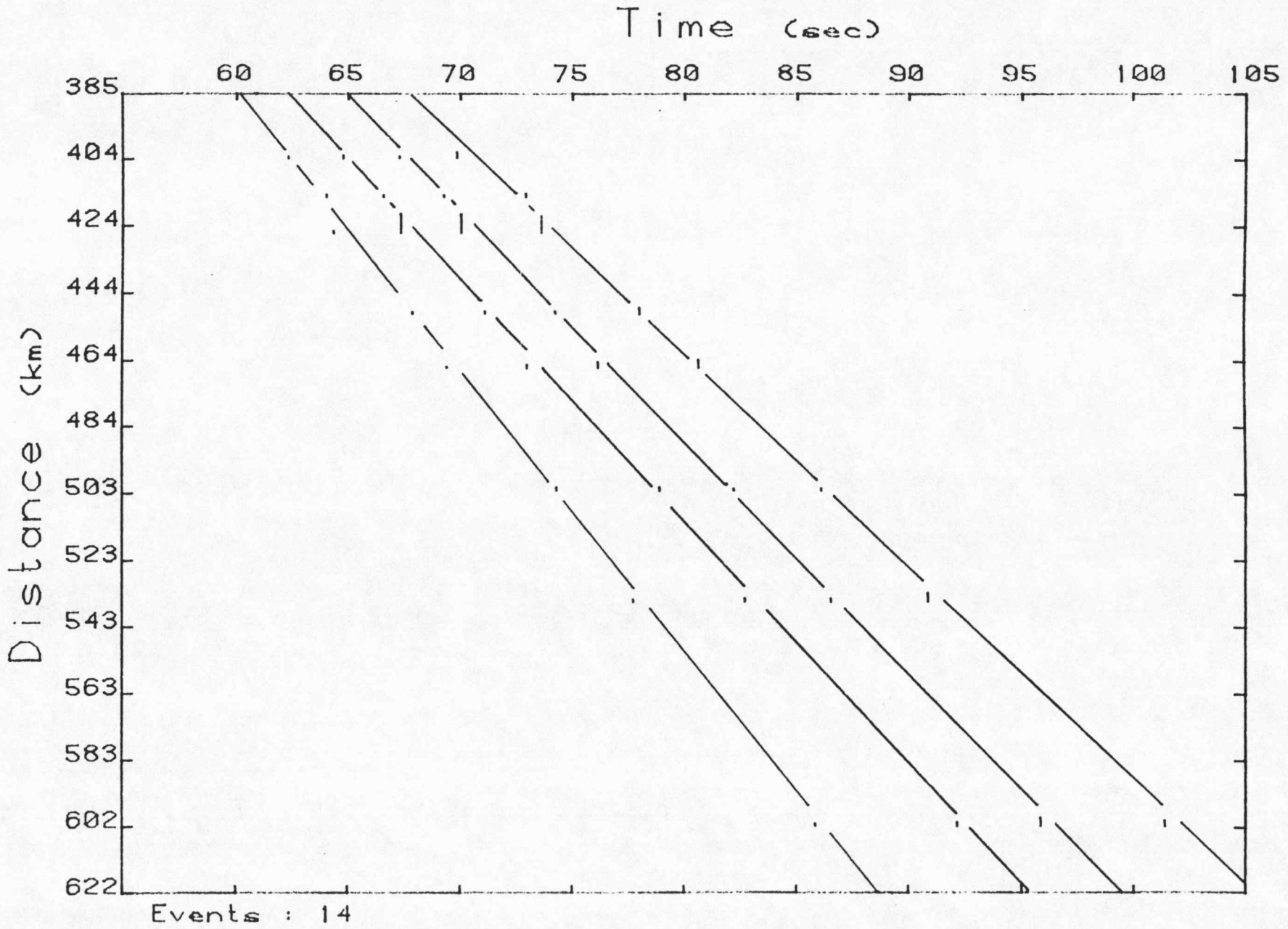
Time (sec)
60
65
70
75
80
85
90
95
100
105
Distance (km)
385
404
424
444
464
484
503
523
543
563
583
602
622
Events : 14

NEBRASKA

May 7, 1978

Event #15

LAT: 42.303°N

LONG: 101.928°W

ORIGIN TIME: 1606:15.9

M_{bLg}: 4.0

DEPTH: 15 km (+2.0 sec)

DIGIT-ORIGIN: 1607:20.0

Station	Epi-Dist	Pn resid	Corrected Pn resid TCK	HWK	EDK	Pn/w	P1/w	P2/w	Pg/w
CNK	471.2	-0.6		-0.4		72.35/2	76.55/2	79.95/2	82.25/1
SNK	521.4	+0.4		+0.4		78.95/1	83.35/3	87.15/2	92.25/1
MLK	553.6	0.0		0.0		82.35/2	88.2/1	91.8/1	96.35/2
HWK	606.7	+0.2		0.0		88.75/2	94.95/0	99.05/1	104.3/1
EMK	640.0	-0.3		-0.4		92.1/2	98.6/1	103.1/2	109.4/2
LAK	672.6	-		-		98.7/4	105.3/2	109.9/2	116.35/3
			VELOCITY (km/sec)			8.54	7.24	6.90	6.13
			Y INTERCEPT (km)			-149.6	-84.0	-79.4	-36.7
			X INTERCEPT (sec)			17.5	11.6	11.5	6.0
			CORRELATION			0.999	0.998	0.998	0.998
			LAYER DEPTH (km)			80.4	57.1	-	-

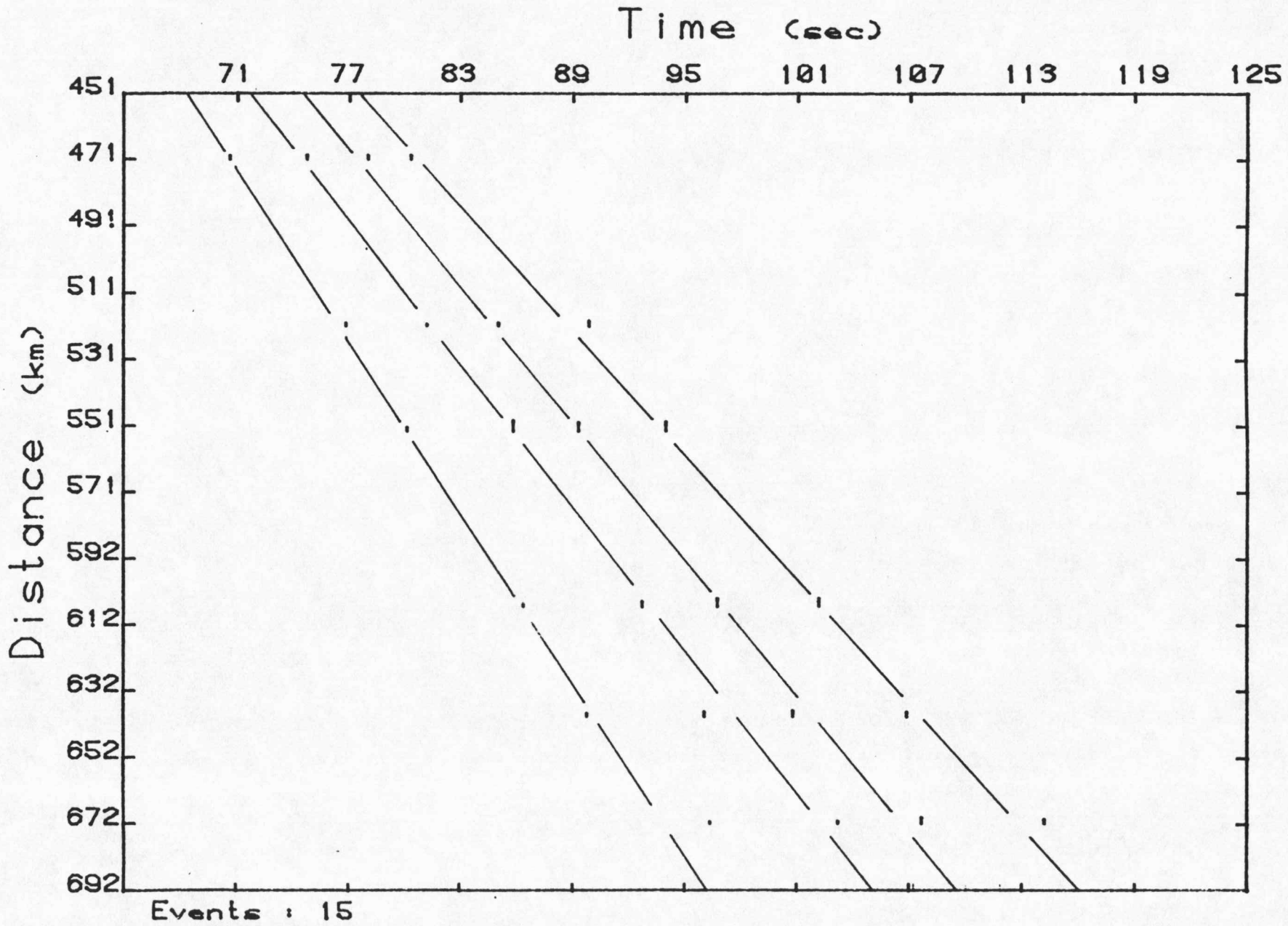
Time (sec)
71
77
83
89
95
101
107
113
119
125
Distance (km)
451
471
491
511
531
551
571
592
612
632
652
672
692
Events : 15

COLORADO

April 2, 1981

Event #16

LAT: 39.910°N

LONG: 104.964°W

ORIGIN TIME: 1610:06.4

M_{bLg}: 4.3

DEPTH: 8.0 km (+1.0 sec)

DIGIT-ORIGIN: 1611:20.0

Station	Epi-Dist	Pn resid	Corrected Pn resid TCK	HWK	EDK	Pn/w	P1/w	P2/w	Pg/w
CNK	621.9	+0.6	+0.5	+0.4	+0.5	86.95/2	91.0/2	95.7/2	102.1/2
SNK	641.1	+0.6	+0.4	+0.4	+0.4	89.10/2	93.35/1	98.15/2	106.15/1
MLK	698.2	-0.8	-0.9	-0.9	-0.9	94.45/2	101.05/2	105.7/3	115.1/1
TCK	708.0	-1.0	-0.8	-1.1	-1.1	95.35/2	102.3/1	107.35/1	117.05/1
EDK	746.2	+0.4	+0.3	+0.3	0.0	101.15/1	109.35/2	115.4/1	124.2/2
BEK	754.5	+1.1	+1.0	+1.0	+1.0	102.85/3	110.9/2	116.45/2	123.45/2
EMK	762.8	+0.3	+0.2	+0.2	+0.2	103.0/2	112.65/2	118.45/2	125.5/2
HWK	808.2	-0.1	-0.2	-0.5	-0.2	107.85/2	118.3/3	122.5/2	132.8/2

VELOCITY (km/sec)	8.59	6.57	6.32	6.14
Y INTERCEPT (km)	-120.3	29.0	23.1	-
X INTERCEPT (sec)	14.0	-4.4	-4.7	-
CORRELATION	0.995	0.997	0.995	0.998
LAYER DEPTH (km)	71.3	-	-	-

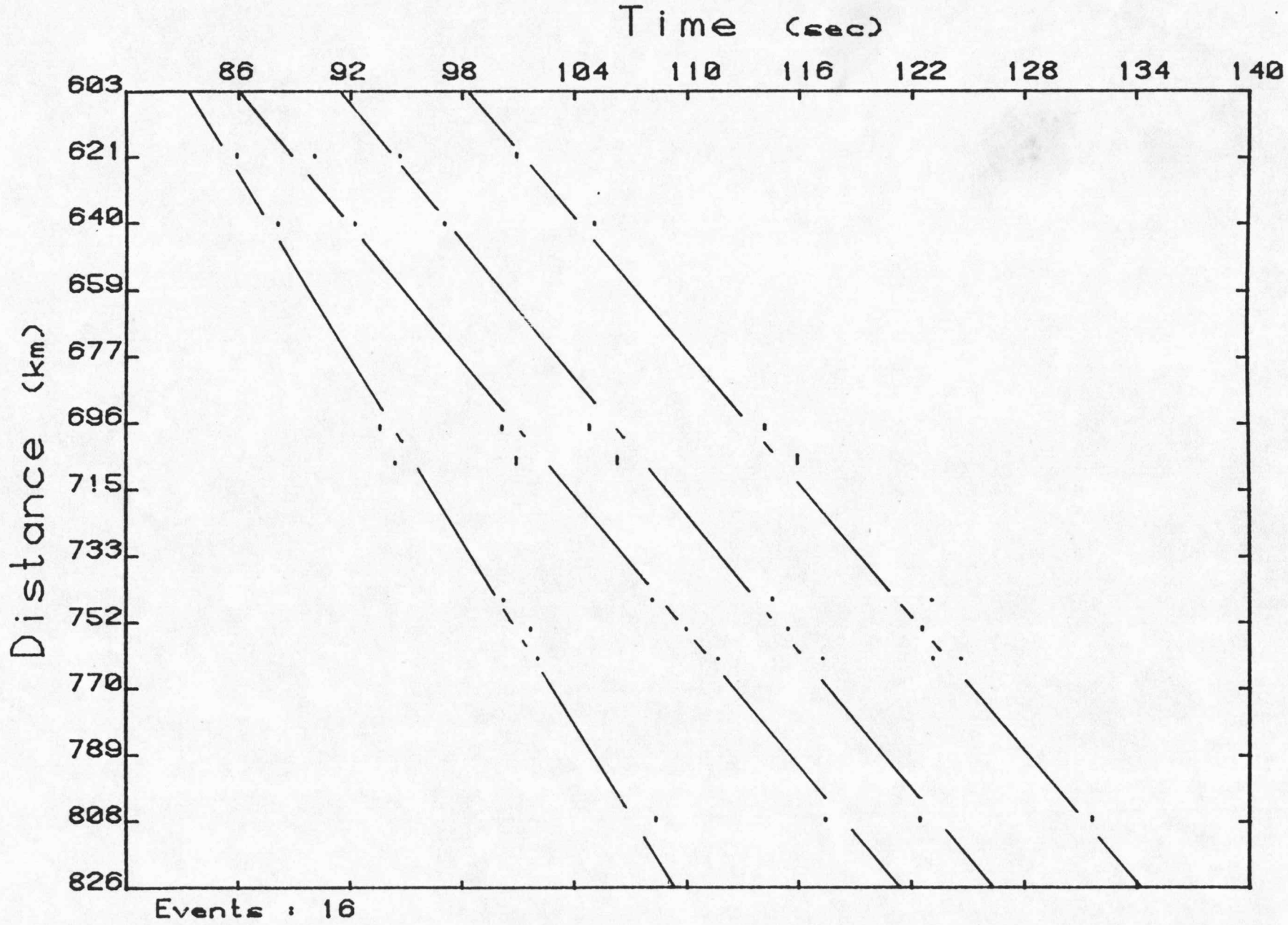
Time (sec)
86
92
98
104
110
116
122
128
134
140
Distance (km)
603
621
640
659
677
696
715
733
752
770
789
808
826
Events : 16